

Point-by-point response

Dear Editor,

Dear associate Editor,

Please find fellow our point-by-point response. Thanks to the valuable comments of the two referees the quality of the manuscript could be improved significantly. Besides improving the description of the model structure and highlighting the novelties of the approach we also expanded our set of reference observations that is used to compare our model and the other two models with obvert annual recharge volumes.

A version of the revised manuscript with all changes marked is provided in the supplement.

We hope that by these changes the manuscript reached a quality that is high enough to be published in Geoscientific Model Development.

Kind regards,

Andreas Hartmann

Referee #1

We thank Dr Long for his valuable review. We performed the following changes on the manuscript according to his specific comments.

Opening paragraph of review: *This manuscript describes a first attempt to estimate groundwater recharge over a regional scale in Europe through the use of a simulation model. The approach presented is novel in that (1) it separates the study area into four karst landscapes by cluster analysis, and (2) the ranges of parameter values were determined by a step-wise process that used observation data and a priori information. Model uncertainty was assessed by evaluating the ranges of model outputs that resulted in the range of Monte Carlo parameter inputs. The manuscript is clearly written, except where noted, and rigorous sand is suitable for publication in GMD after some moderate revisions.*

1. **Referee #1** *The introduction states that a novel approach considers the sub-grid heterogeneity of karst using statistical distribution functions; however, this approach already was used in a previous version, called VarKarst, as described in Section 2.1. The novel parts of the manuscript are outlined in my opening paragraph above and are better described in the Conclusions of the manuscript.*

Answer Indeed, the novel parts of the VarKarst-R model compared to the VarKarst model are not elaborated adequately in the Introduction and the Data and Model section. The revised version of the manuscript highlights now the new functioning of the model just at the beginning of subsection 2.

2. **Referee #1** *Section 2.1 is a brief summary of equations previously published by the Author and appears to be shown here for the purpose of explaining the four parameters. This could be stated*

more clearly because it's not totally clear whether these are new equations or not. Also, the reader would need to read the previous papers to fully understand their meaning. One reason for the confusion is that this is described as being a new version (VarKarst-R), but the equations have not changed (unless I missed something). Therefore, please explain what was modified in the new version.

Answer We agree that a better clarification on the novelties of the VarKarst-R is needed (see our response to the comment just above). In addition, subsection 2.1 that explains the numerical functioning of the model was expanded to achieve better understanding of the model parameters without having to read through the previous papers. This also includes an extra column in Table 2 with a parameter description.

3. **Referee #1** *Section 2.5 states that VarKarst-R simulated recharge was compared to estimates previously published (Table 3); however, table 3 shows only the values estimated by the other studies and not VarKarst-R estimates. I can find no such comparison in this manuscript. It would be very informative to show the VarKarst-R estimated values for these same areas in table 3 for direct comparison.*

Answer The comparison the VarKarst-R simulation results (and the PCR-GLOBWB) results are provided in Figure 9. We apologize for not being clear enough on that. According to comment 2 of referee #2 Table 3 was expanded. Figure 9 and the revised version of the manuscript were updated accordingly. The caption of Figure 9 now includes a reference to the list of references from which the independent recharge amounts were collected (Table 3).

Other comments

1. **Referee #1** *Section 2.3.1, 7894 lines 21-23 – “. . .we assume that differences among the karst landscapes are due to differences in relief and climate, and the consequent processes of landscape evolution including the weathering of carbonate rock.” This neglects several other factors, including depositional environments, tectonics (fracturing), and rain acidity, which could be stated here explicitly. It also could be pointed out that this simple categorization presented seems to be useful nonetheless, and it is also universally applicable and can be objectively applied.*

Answer This is true. We improved the elaborations on the simplifying character of the descriptors used for cluster analysis in the discussion subsection 4.1.1..

2. **Referee #1** *p. 7896 line 5 – What is a reasonable number? Apparently 250 is reasonable because that is the number given later.*

Answer Yes, 250 was regarded to be large enough to provide a reliable measure of spread along with the desired reduction. The respective part was clarified in subsection 2.4.

3. **Referee #1** *p. 7896 lines 8-9 – At first look, a positive correlation seems like a very low threshold C2632 criterion, but when we consider the large uncertainty of recharge estimates, it seems more reasonable. It would be useful to comment briefly on this.*

Answer This rather weak criterion was chosen because the observation data that is available for the parameter confinement strategy can be regarded as uncertain due to differences in scale and the not direct observation of recharge (but recharge related variables as actual evaporation and

soil moisture). We clarified on this point in the revised version of the manuscript at the end of subsection 2.3.2.

4. **Referee #1** p. 7896 lines 19-20 – *In the application of a priori information, it is stated that this assessment would indicate whether or not information applied in steps 1 and 2 is biased. But it does not state what is done if this is the case. Later we see that confinement step 3 is used to further narrow the parameter ranges. Please clarify.*

Answer Step 3 can be regarded as the other 2 previous steps. It is meant to confine the original sample of model parameters. The above-mentioned statement was added because usually a priori information is used first for parameter estimation, before applying observations of the output. Less than usual we chose to add the a priori information at the last step to evaluate the confinement procedure. If confinement steps 1 and 2 would provide completely different ranges than step 3, our procedure (or the data) could be considered flawed. The new version of the manuscript is now providing more detail when explaining confinement step 3 in subsection 2.3.2.

5. **Referee #1** Fig 1a – *This depiction is not clearly explained in the caption or in the manuscript body.*

Answer The caption of Figure 1a is more explanatory is more explanatory now.

6. **Referee #1** Fig 4 – *Please explain AI, DS, and RA.*

Answer The indices AI (aridity index), DS (days of snow) and RA (range of altitudes) are now explained (also in the caption of Table 4).

7. **Referee #1** Fig 5 – *Parameter labels are missing to show the four different columns.*

Answer For each cluster the four columns show the reduction of the complete sample of parameter sets (25,000 x 4 parameters) from the initial sample (light grey) along the 3 confinement steps (moderate grey to black). Hence, the columns do not refer to the individual parameters but to the different step of the confinement procedure. We apologize for being not clear on that. The revised caption of Figure 5 is now more detailed on that.

Referee #2

We thank Dr Hughes for his valuable comments. We prepare to apply his suggestions to improve the manuscript as follows:

1. **Referee #2** *Definition of what geographical area the paper covers. The title says “Europe” but Figure 2 suggests the inclusion of Western Asia, North Africa and the Middle East. Greater clarify as to the geographical zone covered would be appreciated.*

Answer This is true. The simulation domain covers Europe including the Mediterranean. The manuscript title was changed to: “A large-scale simulation model to assess karstic groundwater recharge over Europe and the Mediterranean” and the revised manuscript was adapted accordingly. Only minor parts of the domain may also be attributed to Western Asia and we decided to not mention them explicitly.

2. **Referee #2** *Following on from the above point, given the areal extent of the study, the recharge modelling results culled from the literature is rather limited. A quick literature review of the results*

of recharge modelling in Carbonate aquifers reveals a number of papers:

(...)

These are just a selection and demonstrate that the Table 3 is somewhat limited. Additionally the UK examples are from a very large scale study by Arnell and would benefit again from a more detailed study of the literature.

Answer We agree that a more extensive list of independent studies will improve the quality of the analysis. The list of originally 22 locations from 9 countries was expanded significantly in the revised version of the manuscript especially including some more references within the UK. It now includes 38 locations from 14 countries over Europe and the Mediterranean. Table 3 and Figure 9 were updated accordingly. Unfortunately, 3 of the references suggested by referee #2 could not be used: One of them (Fleury et al., 2007) was already included in the original list in Table 3. The other two (Bakalowicz and Mangion, 2003, and Vilhar et al., 2010) do not provide quantitative information on mean annual recharge volumes, which is needed to evaluate the model.

3. **Referee #2** *The reader is rather rushed into the main part of the paper, and detailed comments are provided below on the introduction. However, it is strongly suggested that to provide a proper context for the equations in Section 2.1 then a basic explanation of the main features of a karst system is provided.*

Answer We agree that the elaboration on the model structure and its novelty compared to the previous version of the model have to be elaborated in more detail. A similar suggestion was given by referee #1. We updated subsection 2.1 accordingly. Please also see our response to comment 1 of referee #1.

4. **Referee #2** *How is river discharge used to calibrate the model? It is mentioned at the start of the paper (line 7, pg 7890), but not addressed. Given the lack of runoff in Karst regions, can this be used as calibration parameter?*

Answer We used observed soil moisture time series from the International Soil Moisture Network (ISMN) and observed actual evaporation time series from FLUXNET as recharge related observations since discharge observations are not available (as correctly stated by referee #2). To account for that, and uncertainties that go along with the differences of observation and simulation scale, we defined rather weak parameter selection criterions in our parameter confinement procedure (please also see our response to *Other Comment 3* of referee #1)

Specific comments

5. **Referee #2** P7888 L 24 Change “regions constitute” to “regions only constitute”

Answer Done

6. **Referee #2** P 7888 L 25 Change “yet up to 50%” to “yet contribute up to 50%”

Answer Done

7. **Referee #2** P 7889 L 1-3 Add in sentence before “Climate simulations....(Christensen et al.,2007)”to introduce topic

Answer Done.

8. **Referee #2** P 7889 L 5 Add explanation of impact after “can be expected”

Answer Done.

9. **Referee #2** P 7889 L 5-6 Clarify size of regional models as in groundwater modelling the scale is 1000-10000 km²

Answer Done.

10. **Referee #2** P 7889 L 8 Change “predictions derive” to “predictions should derive”

Answer Done.

11. **Referee #2** P 7889 L 11 Change “presently available” to “Currently available”

Answer Done.

12. **Referee #2** P 7889 L 19 Add description of scientific discourse after “scientific discourse”

Answer Done.

13. **Referee #2** P 7889 L 28 “a priori” to be italicised (Latin not English) – same for “posterior” elsewhere

Answer Done.

14. **Referee #2** P 7890 L 1 Change “dynamics prohibited” to “dynamics have prohibited”

Answer Done.

15. **Referee #2** P 7890 L 7 Change “and river discharge” to “as well as river discharge”

Answer Done.

16. **Referee #2** P 7890 L 14 “vertical recharge” this not a regularly used term within the literature, so would benefit from a better explanation or use “actual recharge” is you mean the recharge that reaches the water table

Answer “vertical recharge” was replaced by “potential recharge”, which from our point of view represents best the simulated variable, because on its path downwards water could still be diverge by impermeable materials before it can reach the groundwater table to become “actual recharge”.

17. **Referee #2** P 7894 L 1 Charge “from FLUXNET” to “from the FLUXNET observation network”

Answer Done.

18. **Referee #2** P 7895 L 1 Change “clusteranalysis” to “cluster analysis”

Answer Done.

19. **Referee #2** P 7896 L 4 Change “trial-and-error reducing the initial sample” to “trial-and-error which reduced the initial sample”

Answer Done.

20. **Referee #2** P 7898 L 22 Change “medium range mountains show” to “medium range mountains (MED) show”

Answer Done.

21. **Referee #2** P 7898 L 23 Change “Desert hills and plains are” to “Desert hills and plains (DES) are”

Answer Done.

22. **Referee #2** P 7899 L 3 Add an explanation as to Greece and Turkey have both HUM and DES in close proximity; something like “Where mountainous regions are in close proximity to the coast”

Answer Done.

23. **Referee #2** P 7900 L 10 Northern Africa isn’t in Europe (see general comments above and title of the paper)

Answer By changing the description of the model area to “Europe and the Mediterranean” we solved this contradiction.

24. **Referee #2** P 7902 L 18 Remove “as”

Answer Done.

25. **Referee #2** P 7902 L 19 Change “Transitions” to “Typically transitions”

Answer Done.

26. **Referee #2** P 7902 L 19 Remove “rather”

Answer Done.

27. **Referee #2** P 7902 L 21 Change “transient,” to “graded”

Answer Done.

28. **Referee #2** P 7902 L 28 Change “the correlation” to “the order of the correlation”

Answer Done.

29. **Referee #2** P 7903 L 1 Remove “in their order”

Answer Done.

30. **Referee #2** P 7903 L 2 Change “the other order” to “the alternative order”

Answer Done.

31. **Referee #2** P 7903 L 3 Change “indicating similar” to “indicating the similar”

Answer Done.

32. **Referee #2** P 7904 L 21 Change “recharge volumes” to “recharge rates”

Answer “recharge volumes” was replaced by “recharge amounts” because in some fields “recharge rate” is defined as the fraction of precipitation that becomes recharge [%].

33. **Referee #2** P 7904 L 24 Is it Northern UK or Northern England (as in line 9 pg 7900)? This difference is important to Scottish readers!

Answer It is Northern UK. The text was corrected accordingly.

34. **Referee #2** P 7905 L 19 Change “content of the” to “contained in the”

Answer Done.

35. **Referee #2** P 7906 L 22-23 Two uses of the word “additional” in the same sentence – choose another

Answer the first “additional” was replaced by “combined”.

36. **Referee #2** P 7906 L 26 Change “distribution parameter” to “parameter distribution”

Answer in this sentence we wanted to refer to the model parameter α but we created confusion by not using its defined name “variability constant”. This error is corrected now.

37. **Referee #2** P 7907 L 3 Change “elaborates” to “elaborate”

Answer Done.

38. **Referee #2** P 7907 L 5 Change “this study” to “this paper”

Answer Done.

39. **Referee #2** P 7907 L 16 Change “does not exist” to “is not generated”

Answer Done.

40. **Referee #2** P 7907 L 19 Change “therefore” to “subsequently”

Answer Done.

41. **Referee #2** P 7908 L 3 Change “contribute” to “consists of”

Answer “contribute” was changed to “comprise”.

42. **Referee #2** P 7908 L 7 Change “present” to “current”

Answer W

43. **Referee #2** P 7908 L 11 Change “over-estimation” to “over-estimation of recharge”

Answer Done.

44. **Referee #2** P 7908 L 12 Change “financial resources excessive investments into drinking water” to “financial resources the excessive investment in ensuring the security of drinking water supply”

Answer Done.

45. **Referee #2** P 7908 L 16 Change “we presented” to “we have presented”

Answer Done.

46. **Referee #2** P 7908 L 24 Change “present” to “current”

Answer Done.

47. **Referee #2** P 7909 L 8 Change “prone” to “liable”

Answer Done.

48. **Referee #2** P 7909 L 14 Change “than the inflow and pumping” to “than just the inflow. Further pumping”

Answer Done.

49. **Referee #2** P 7909 L 19 Change “Strub from the Chair of Hydrology” to “Strub, Professor of Hydrology

Answer the sentence was changed to “... Strub, research associate at the Chair of ...”.

A large-scale simulation model to assess karstic groundwater recharge over Europe and the Mediterranean ~~simulation model to assess groundwater recharge over Europe's karst regions~~

A. Hartmann^{1,3}, Tom Gleeson², Rafael Rosolem¹, Francesca Pianosi¹, Yoshihide Wada⁴, Thorsten Wagener¹

[1] Department of Civil Engineering, University of Bristol, United Kingdom

[2] Civil Engineering, McGill University, Canada

[3] Faculty of Environment and Natural Resources, University of Freiburg, Germany

[4] Department of Physical Geography, Utrecht University, The Netherlands

Correspondence to: A. Hartmann (aj.hartmann@bristol.ac.uk)

~~ReS~~submitted to Geoscientific Model Development ~~September~~ March 2015~~4~~

Abstract

Karst develops through the dissolution of carbonate rock and is a major source of groundwater contributing up to half of the total drinking water supply in some European countries. Previous approaches to model future water availability in Europe are either too-small scale or do not incorporate karst processes, i.e. preferential flow paths. This study presents the first simulations of groundwater recharge in all karst regions in Europe with a parsimonious karst hydrology model. A novel parameter confinement strategy combines *a priori* information with recharge-related observations (actual evapotranspiration and soil moisture) at locations across Europe while explicitly identifying uncertainty in the model

parameters. Europe's karst regions are divided into 4 typical karst landscapes (humid, mountain, Mediterranean and desert) by cluster analysis and recharge is simulated from 2002 to 2012 for each karst landscape. Mean annual recharge ranges from negligible in deserts to >1 m/a in humid regions. The majority of recharge rates ranges from 20%-50% of precipitation and are sensitive to sub-annual climate variability. Simulation results are consistent with independent observations of mean annual recharge and significantly better than other global hydrology models that do not consider karst processes (PCR-GLOBWB, WaterGAP). Global hydrology models systematically underestimate karst recharge implying that they over-estimate actual evapotranspiration and surface runoff. Karst water budgets and thus information to support management decisions regarding drinking water supply and flood risk are significantly improved by our model.

1 Introduction

Groundwater is the main source of water supply for billions of people in the world (Gleeson et al., 2012). Carbonate rock regions only constitute about 35% of Europe's land surface (Williams and Ford, 2006), yet contribute up to 50% of the national water supply in some European countries (COST, 1995) because of their high storage capacity and permeability (Ford and Williams, 2007). Climate conditions have a primary control on groundwater recharge (de Vries and Simmers, 2002). Climate simulations suggest that in the next 90 years Mediterranean regions will be exposed to higher temperatures and lower precipitation amounts (Christensen et al., 2007). In addition, shifts in hydrological regimes (Milly et al., 2005) and hydrological extremes (Dai, 2012; Hirabayashi et al., 2013) can be expected. To assess the impact of climate change on regional groundwater resources as groundwater depletion or deteriorations of water quality, large-scale simulation models are necessary that go beyond the typical scale of aquifer simulation models (~10-10,000 km²). –Additionally, we expect the future variability of climate to be beyond that reflected in historical observations, which means that model predictions should derive credibility via more in-depth diagnostic evaluation of the consistency between the model and the underlying system and not from some calibration exercise (Wagener et al., 2010).

Presently–Currently available global hydrology models discretise the land surface in grids with a resolution down to 0.25 to 0.5 decimal degrees. Parts of the vertical fluxes are well represented, e.g. the energy balance (Ek, 2003; Miralles et al., 2011). But groundwater

recharge and groundwater flow are represented simply by heuristic equations (Döll and Fiedler, 2008a) or assumptions of linearity (Wada et al., 2010, 2014). They do not explicitly simulate a dynamic water table or regional groundwater flow. Global models also assume homogenous conditions of hydrologic and hydraulic properties in each of their grid cells, rather than variable flow paths, and they completely omit the possibility of preferential flow. This was criticized in the recent scientific discourse about the need for large-scale hyper-resolution models (Beven and Cloke, 2012; Wood et al., 2011).

The assumption of homogeneity is certainly inappropriate for karst regions. Chemical weathering of carbonate rock and other physical processes develop preferential pathways and strong subsurface heterogeneity (Bakalowicz, 2005). Flow and storage are heterogeneous ranging from very slow diffusion to rapid concentrated flow at the surface, in the soil, the unsaturated zone and the aquifer (Király, 1998). A range of modeling studies have developed and applied karst specific models at individual karst systems at the catchment or aquifer scale (Doummar et al., 2012; Fleury et al., 2007; Hartmann et al., 2013b; Le Moine et al., 2008) but a lack of *a priori* information of aquifer properties and observations of groundwater dynamics have prohibited their application on larger scales (Hartmann et al., 2014a).

Compared to the limited information about the deeper subsurface there is much better information about the surface and shallow subsurface including maps of soil types and properties (FAO/IIASA/ISRIC/ISSCAS/JRCv, 2012), observations of soil moisture (International Soil Moisture Network, Dorigo et al., 2011) and of latent heat fluxes (FluxNet, Baldocchi et al., 2001), and-as well as river discharge (GRDC, 2004). Surface and shallow subsurface information is used for the parameterization and evaluation of the surface routines of present large-scale models. But, although these data also cover Europe's karst regions, it has not been used for the development of large-scale models to simulate karstic surface and shallow subsurface flow and storage dynamics.

The objective of this study is to develop the first large-scale simulation model for karstic groundwater recharge over Europe and the Mediterranean~~in Europe's karst regions~~. Despite much broader definitions of groundwater recharge (e.g., Lerner et al., 1990), we focus on vertical-potential recharge, that is -vertical percolation from the soil below the depth affected by evapotranspiration. We use a novel type of model structure that considers the sub-grid heterogeneity of karst properties using statistical distribution functions. To achieve a realistic parameterization of the model we identify typical karst landscapes by cluster analysis and by

a combined use of *a priori* information about soil storage capacities and observations of recharge related fluxes and storage dynamics. Applying a parameter confinement strategy based on Monte Carlo sampling we are able to provide large-scale simulations of annual recharge ~~over Europe's karst regions~~ including a quantification of their uncertainty.

2 Data and Methods

2 Due to chemical weathering (karstification) karst systems have a strong subsurface heterogeneity of flow and storage processes (Bakalowicz, 2005) that have to be considered to produce realistic simulations (Hartmann et al., 2014a). In this study, large-scale karst recharge is estimated by a modified version of the VarKarst model (Hartmann et al., 2013a), called VarKarst-R from here, on a 0.25 x 0.25 decimal degree grid. The model has shown to be applicable at various scales and climates over Europe (Hartmann et al., 2013b). To apply the model on a large scale we developed a new parameter estimation procedure that separates the study area into four karst landscapes by cluster analysis and estimates model parameters and their uncertainty by a step-wise parameter confinement process.

2.1 The model

~~Due to chemical weathering (karstification) karst systems have a strong subsurface heterogeneity of flow and storage processes (Bakalowicz, 2005) that have to be considered to produce realistic simulations (Hartmann et al., 2014a). In this study, large-scale karst recharge is estimated by a modified version of the VarKarst model (Hartmann et al., 2013a), called VarKarst-R from here, on a 0.25 x 0.25 decimal degree grid. The model has shown to be applicable at various scales and climates over Europe (Hartmann et al., 2013b). The VarKarst-R model simulates potential recharge, which is the water column the vertically percolated from the soil and epikarst. Hence, the previous version of the model is reduced to include only the soil and the epikarst simulation routines but still using the same~~ Its main advantage includes the capability to represent subsurface heterogeneity using statistical distribution functions allowing that allow for variable soil depths, variable epikarst depths and variable subsurface dynamics (Figure 1~~Figure 1~~). This leads to a parametrically efficient process representation. Comparisons with independently derived field data showed that these distribution functions are a good approximation of the natural heterogeneity (Hartmann et al., 2014b).

Heterogeneity of soil depths is represented by a mean soil storage capacity V_{soil} [mm] and a ~~distribution variability coefficient constant~~ a [-]. The soil storage capacity $V_{S,i}$ [mm] for every compartment i is defined by:

$$V_{S,i} = V_{\max,S} \cdot \left(\frac{i}{N} \right)^a \quad (1)$$

where $V_{\max,S}$ [mm] is the maximum soil storage capacity and N is the total number of model compartments. This is derived from the mean soil storage capacity V_{soil} as

$$\int_0^{i_{1/2}} V_{\max,S} \left(\frac{x}{N} \right)^a dx = \frac{\int_0^N V_{\max,S} \left(\frac{x}{N} \right)^a dx}{2}; V_{soil} = V_{\max,S} \left(\frac{i_{1/2}}{N} \right)^a$$

$$\Downarrow$$

$$V_{\max,S} = V_{soil} \cdot 2^{\left(\frac{a}{a+1} \right)} \quad (2)$$

where $i_{1/2}$ is the compartment at which the soil storage capacities on the left equal the soil storage capacities on the right ([Figure 1](#)~~Figure 1~~a). Preceding work (Hartmann et al., 2013a, 2013b) showed that the same distribution coefficient a can be used to derive the epikarst storage distribution $V_{E,i}$ from the mean epikarst storage capacity V_{epi} [mm] (via the maximum epikarst storage $V_{\max,E}$ likewise to $V_{\max,S}$ in Eq (2)):

$$V_{E,i} = V_{\max,E} \cdot \left(\frac{i}{N} \right)^a \quad (3)$$

At each time step t , the actual evapotranspiration from each soil compartment $E_{act,i}$ is found by:

$$E_{act,i}(t) = E_{pot}(t) \cdot \frac{\min[V_{soil,i}(t) + P_{eff}(t) + Q_{surface,i}(t), V_{S,i}]}{V_{S,i}} \quad (4)$$

where E_{pot} [mm] is the potential evapotranspiration derived by the Priestley-Taylor equation (Priestley and Taylor, 1972), P_{eff} [mm] is the sum of liquid precipitation and snow melt, $Q_{surface,i}$ [mm] is the surface inflow arriving from compartment $i-1$ (see Eq. (9)), and $V_{S,i}$ [mm] the water stored in the soil at time step t . Snow fall and snow melt are derived from daily snow water equivalent available from GLDAS-2 ([Table 1](#)~~Table 1~~). During days with snow cover we set $E_{act}(t)=0$. Flow from the soil to the epikarst $R_{Epi,i}$ [mm] is calculated by:

$$R_{Epi,i}(t) = \max[V_{Soil,i}(t) + P_{eff}(t) + Q_{Surface,i}(t) - E_{act,i}(t) - V_{S,i}, 0] \quad (5)$$

Following an assumption of linearity (Rimmer and Hartmann, 2012), the epikarst storage coefficients $K_{E,i}$ [d] controls the epikarst outflow dynamics:

$$Q_{Epi,i}(t) = \frac{\min[V_{Epi,i}(t) + R_{Epi,i}(t), V_{E,i}]}{K_{E,i}} \cdot \Delta t \quad (6)$$

$$K_{E,i} = K_{Epi} \cdot \left(\frac{N-i+1}{N} \right)^a \quad (7)$$

where $V_{E,i}$ [mm] is the water stored in compartment i of the epikarst at time step t . Again, the same distribution coefficient a is applied to derive $K_{E,i}$ from [the mean epikarst storage coefficient](#) $K_{max,Epi}$. The latter is obtained from the mean epikarst storage coefficient K_{epi} using:

$$\begin{aligned} N \cdot K_{mean,E} &= \int_0^N K_{max,E} \left(\frac{x}{N} \right)^a dx \\ &\Downarrow \\ K_{max,E} &= K_{epi} \cdot (a+1) \end{aligned} \quad (8)$$

When infiltration exceeds the soil and epikarst storage capacities, surface flow to the next model compartment $Q_{Surf,i+1}$ [mm] initiates:

$$Q_{Surf,i+1}(t) = \max[V_{Epi,i}(t) + R_{Epi,i}(t) - V_{E,i}, 0] \quad (9)$$

To summarize, the model is completely defined by the four parameters a , K_{epi} , V_{soil} , and V_{epi} ([Table 2Table 2](#)).

2.2 Data availability

Forcing for the VarKarst-R model is derived through the Global Land Data Assimilation System (GLDAS-2) that assimilates satellite- and ground-based observational data products to obtain optimal fields of land surface states and fluxes (Rodell et al., 2004; Rui and Beaudoin, 2013). While precipitation, temperature and net radiation are mainly merged from satellite and gauge observations, snow water equivalent is derived using data assimilation as well as the snow water equivalent simulations of the NOAH land surface model v3.3 (Ek, 2003) driven by GLDAS-2 forcing. Europe's [and the Mediterranean's](#) carbonate rock areas are

derived from a global map (vector data) of carbonate rock (Williams and Ford, 2006). Each cell of the 0.25 decimal degree simulation grid intersecting a carbonate rock region was considered a karst region. The model was calibrated and evaluated with observations of actual evapotranspiration from [the FLUXNET](#) (Baldocchi et al., 2001) and with soil water content data from the International Soil Moisture Network ISMN (Dorigo et al., 2011). Only stations within carbonate rock regions and with ≥ 12 months of available data were used ([Figure 2](#)). Months with < 25 days of observations were discarded. In addition, months with $\geq 50\%$ mismatch in their energy closure were discarded from the FLUXNET data set (similar to Miralles et al., 2011).

2.3 Parameter estimation

A lack of *a priori* information and observations of discharge and groundwater levels that can be used for calibration are the primary reasons why karst models have not been applied on larger scales yet (Hartmann et al., 2014a). The parameter assessment strategy we present in the following is meant to overcome this problem by using a combination of *a priori* information and recharge-related variables. We define typical karst landscapes over Europe [and the Mediterranean](#) and apply this combined information to a large initial sample of possible model parameter sets. In a step-wise process we then discard all parameter sets that produce simulations inconsistent with our *a priori* information and our recharge-related observations.

2.3.1 Definition of typical karst landscapes

Our definition of typical karst landscapes is based on the well-known the hydrologic landscape concept (Winter, 2001), which describes hydrological landscapes based on their geology, relief and climate. Constraining ourselves to karst regions that mainly develop on carbonate rock we assume that differences among the karst landscapes are due to differences in relief and climate, and the consequent processes of landscape evolution including the weathering of carbonate rock (karstification). [Europe's The](#) carbonate rock regions [in Europe and the Mediterranean](#) are divided into typical landscapes using simple descriptors of relief (range of altitude [RA](#)) and climate (aridity index [AI](#) and mean annual number of days with snow cover [DS](#)) within each of 0.25 decimal degree grid cells and a standard-cluster analysis scheme (k-means method). We test the quality of clustering for 2 to 20 clusters by calculating the sums of squared internal distances to the cluster means. The so-called “elbow method”

identifies the point where adding additional clusters only leads to a marginal reduction in the internal distance metric, i.e. the percentage of variance explained by adding more clusters would not increase significantly (Seber, 2009).

2.3.2 Model parameters for each karst landscape

We initially sample 25,000 possible model parameter sets from independent uniform distributions using parameter ranges derived from previous catchment scale applications of the VarKarst-R model over Europe and the Mediterranean (Table 2Table-2). We use *a priori* information and recharge-related observations to assess parameter performance for each karst landscape. *A priori* information consists of spatially distributed information about mean soil storage capacities as provided by several preceding mapping and modelling studies (Ek, 2003; FAO/IIASA/ISRIC/ISSCAS/JRCv, 2012; Miralles et al., 2011). Recharge-related variables are (1) soil moisture observations and (2) observations of actual evaporation at various locations over Europe—the modelling domain (Table 1Table-1, Figure 2Figure-2). Soil moisture is related to recharge because it indicates the start and duration of saturation of the soil during which diffuse and preferential recharge can take place. Actual evaporation is related to recharge because usually no surface runoff occurs in karst regions due to the high infiltration capacities (Jeannin and Grasso, 1997). The difference of monthly precipitation and actual evaporation is therefore a valid proxy for groundwater recharge at a monthly time scale or above. The new parameter confinement strategy is applied to each of the karst landscapes in 3 steps:

1. Bias rule: retain only the parameter sets that produce a bias between observed and simulated actual evaporation lower than 75% at all FLUXNET locations within the chosen karst landscape:

$$\min_i(bias_i) = \min_i \left(\frac{\mu_{sim,i} - \mu_{obs,i}}{\mu_{obs,i}} \right) < 75\% \quad (10)$$

Where $m_{sim,i}$ and $m_{obs,i}$ are the sum of simulated and observed actual evapotranspiration at location i , respectively. The value 75% was found by trial-and-error, which reduced ~~reducing~~ the initial sample to a reasonable number. The bias rule was not applied on the soil moisture since porosities of the soil matrix were not available prohibiting a comparison of simulated and observed soil water contents.

2. Correlation rule: retain only the parameter sets that produce a positive coefficient of (Pearson) correlation between observations and simulations of both actual evaporation and soil moisture, at all locations:

$$\left(\min_i [corr(AET_{sim,i}, AET_{obs,i})] \wedge \min_j [corr(\theta_{sim,j}, \theta_{obs,j})] \right) > 0 \quad (11)$$

where $AET_{sim,j}$ and $AET_{obs,j}$, and $\theta_{sim,j}$ and $\theta_{obs,j}$ are the monthly means of simulated and observed actual evapotranspiration, and soil water content at locations i/j , respectively.

3. Application of *a priori* information: retain only parameter sets in which V_{soil} falls within the feasible ranges that can be derived from *a priori* information about the maximum soil storage capacity in different karst landscapes (Ek, 2003; FAO/IIASA/ISRIC/ISSCAS/JRCv, 2012; Miralles et al., 2011). Less than usual ~~We~~ add the *a priori* information at the last step to evaluate if the *posterior* distributions of V_{soil} already adapt to the ranges defined in this confinement step. If they do not we would conclude that the recharge related information applied in confinement steps 1 and 2 is biased. If they do, we have indication that the data applied in all 3 steps is complementary.

Each step reduces the initial parameter sample differently for each of the karst landscapes. The *posterior* parameter distributions within the confined samples should be different among the karst landscapes if the karst landscapes are properly defined. The rather weak thresholds in step 1 and 2 were chosen to take into account the uncertainties resulting from the differences in scales of observations (point) and simulations (grid cell), and from the indirect observation of recharge (actual evaporation and soil moisture as recharge related variables).

2.4 Recharge simulations over Europe and the Mediterranean

Recharge is simulated over the carbonate regions of Europe and the Mediterranean from 2002/03 to 2011/12 using the confined parameter samples for each of the identified karst landscapes and the available forcings (Table 1~~Table 1~~). The mean and standard deviation of simulated recharge for each grid cell and time step is calculated by uniform discrete sampling of a representative subset of 250 parameter sets from each of the confined parameters sets which we regarded to be large enough to provide a reliable measure of spread.

2.5 Model evaluation

To assess the realism of simulated groundwater recharge we compare simulated with observed mean annual recharge volumes derived independently from karst studies over Europe and the Mediterranean (Table 3~~Table 3~~). In addition, we compare our results to the simulated mean annual recharge volumes of two well-established global simulation models: PCR-GLOBWB (Wada et al., 2010, 2014) and WaterGAP (Döll and Fiedler, 2008a; Döll et al., 2003).

We furthermore apply a global sensitivity analysis strategy, called Regional Sensitivity Analysis (Spear and Hornberger, 1980), to evaluate the importance of the 4 model parameters at different simulation time scales ranging from 1 month up to 10 years. This analysis shows (1) which simulated process and characteristics are dominant at a given time scale and (2) which parameters will need more careful calibration when the model will be used in future studies. We use the same sample of 25,000 parameter sets that was created for the parameter estimation strategy (subsection 2.3.2) and assess the sensitivity of 4 model outputs representative of different time scales: coefficient of variation (CV) of simulated monthly recharge volumes (monthly), CV of simulated 3-monthly recharge volumes (seasonal), CV of annual recharge volumes (annual), and total recharge over the entire 10-year simulation period (decadal). We do not consider temporal resolution less than a month given the assumption that the difference of precipitation and actual evapotranspiration can be a proxy for groundwater recharge, and due to uncertainties related to differences in simulation (grid cell) and observation (point).

For each of the identified karst landscapes we choose the 10 locations that are closest to their cluster means (Euclidean distances to relief and climate descriptors; subsection 2.3.1) as representative locations. In the regional sensitivity analysis approach, we split the parameter sets into two groups, those that produce simulations above the simulated median of one of the 4 model outputs and those that produce simulations below. We then calculate the maximum distance $D(x)$ between marginal cumulative distribution functions (CDFs) produced by these two distributions for each of the parameters – a large distance $D(x)$ suggests that the parameter is important for simulating this particular output (Figure 3~~Figure 3~~).

3 Results

3.1 Parameter assessment

3.1.1 Definition of typical karst landscapes

Cluster analysis resulted in four clusters, which are generally spatially contiguous ([Figure 4](#)) and have quantitatively distinct cluster means ([Table 4](#)). We can attribute particular characteristics to each cluster using the mean values of the clustering descriptors ([Table 4](#)): (1) Humid hills and plains (HUM) are characterised by an aridity index <1 , a significant number of days with snow cover and low elevation differences. (2) High range mountains (MTN) have an aridity index of ~ 1 , they also have a significant number of days with snow cover and they show very large topographic elevation differences. (3) Mediterranean medium range mountains ([MED](#)) show a high aridity index, only few days with snow cover and high elevation differences. (4) Desert hills and plains ([DES](#)) are described by similar altitude ranges as the humid hills and plains but they have a high aridity indices and almost no days with snow cover. The karst landscapes order from North (HUM) to South (DES) based on increasing temperatures and decreasing precipitation amounts. While HUM and DES appear to be separated clearly, MTN and MED mix in some regions, for instance Greece and Turkey where mountainous regions are in close proximity to the coast.

3.1.2 Model parameter estimates for each karst landscape

The three steps of the new parameter confinement strategy resulted in a significant reduction of the initial sample of 25,000 parameter sets ([Figure 5](#)). Each step has a different impact on the reduction among the identified landscapes. For the humid karst landscapes, the correlation rule appears to have the strongest impact while for the mountain and Mediterranean landscapes the bias rule results in the strongest reduction. For the desert landscape only step 3, i.e. application of *a priori* information, reduces the initial sample because no data was available to apply steps 1 and 2. Considering the parameter ranges for each landscape after the application of the confinement strategy ([Table 5](#)), we only achieved a confinement of the distribution parameter a , the soil storage capacity V_{soil} , and slight confinement of the epikarst storage coefficient K_{epi} .

The impact of the three confinement steps becomes more obvious when considering their *posterior* distributions (Figure 6). The distributions of parameters a , K_{epi} and V_{soil} evolve significantly away from their initial uniform distributions along the confinement steps. In general, changes of the *posterior* distributions of each landscape's parameter samples are in accordance with the reductions of their number (Figure 5), though changes are pronounced differently among the parameters. While a and V_{soil} change strongly for HUM, MTN and MED, V_{epi} maintains a uniform distribution across all steps. K_{epi} also exhibits strong changes for HUM but they are less pronounced for MTN and MED. The *posterior* distributions of the DES landscape do not change except for step 3 due to the lack of information to apply confinement steps 1 and 2. Step 3 results in a tailoring of the distribution of V_{soil} for all landscapes. For HUM, MTN and MED it can be seen that confinement steps 1 and 2 already pushed the parameter distributions towards their final shape, meaning that the changes in parameter distributions induced by the comparison with observations are consistent with the *a priori* information about the physical characteristics of the karst.

3.2 Recharge simulations over Europe and the Mediterranean

The parameter confinement strategy allows us to apply VarKarst-R over all of Europe and the Mediterranean, and to obtain recharge simulations for the hydrological years 2002/03-2011/12. Thanks to the 250 parameter sets that we samples from the *posterior* parameter distributions we can include an estimate of uncertainty for each grid cell (Figure 7). Mean annual recharge ranges from almost 0 to >1000 mm/a with the highest volumes found in Northern EnglandUK, the Alps and former Yugoslavia. The lowest values are found in the desert regions of Northern Africa. The vast majority of recharge rates ranges from 20%-50% of precipitation. Considering the simulations individually for each karst landscape reveals that the mountain landscapes produce the largest recharge volumes followed by the humid and Mediterranean landscapes (Figure 8a). The desert landscapes produce the lowest recharge volumes. However, the recharge rates reveal that on average the Mediterranean landscapes show the largest recharge rates, followed by the highly variable mountains (Figure 8c). Humid and deserts landscapes exhibit lower recharge rates. Uncertainties, expressed by the standard deviation of the 250 simulations for each grid cell, are rather low, seldom exceeding 35 mm/a (Figure 8b). However, expressed as coefficients of variation, most of them range from 5%-25% for the humid, mountain and Mediterranean

landscapes but for the desert landscape they can reach up to 50% of the mean annual recharge (Figure 8d).

3.3 Model evaluation

We compare the simulated recharge volumes of our model with recharge volumes assessed from independent and published karst studies over Europe and the Mediterranean (Figure 9a). Even though there is a considerable spread across the simulations their bulk plots well around the 1:1 line achieving an average deviation of only -22 mm/a (Table 6). Considering the individual karst landscapes there is an over-estimation of recharge for the humid landscapes and an under-estimation for the mountain landscapes. The best results are achieved for the Mediterranean landscapes with only slight under-estimation (Figure 9a). When we compare the same observations to the simulated recharge volumes of the PCR-GLOBWB (Figure 9b) and WaterGAP models (Figure 9c) we find a strong tendency of under-estimation that is strongest for the mountain and Mediterranean landscapes but still significant for the humid landscapes (Table 6). For the humid landscapes absolute deviations are similar among the three models.

In addition to comparing simulated and observed annual averages, sensitivity analysis on the model output gives us insight in the realism of the model and the importance of individual model parameters at different time scales (Figure 10). Our results show that parameters a and V_{soil} have the overall strongest influence on the simulated recharge from a monthly to a 10-year time scale but their influence decreases toward shorter time scales. Simultaneously the epikarst parameter K_{epi} gains more importance. This behaviour is most pronounced for the Mediterranean and desert landscapes. The same is true for V_{epi} , but its overall importance remains much lower, which was also found in the parameter confinement strategy (Figure 6).

4 Discussion

4.1 Reliability of parameter estimation

4.1.1 Identification of karst landscapes

The identification of different karst landscapes is a crucial step within our new parameter estimation strategy. The four karst landscapes we identified depend mostly on the choice of

climatic and topographic descriptors (~~Table 4~~~~Table 4~~) and the selected number of clusters. ~~Even though neglecting several factors as depositional environments, fracturing by tectonic processes or regional variations in rain acidity~~ ~~The our~~ choice of descriptors is well justified from our understanding of dominant hydrologic process controls as formalized in the hydrologic landscape concept (Winter, 2001) and applied similarly at many other studies (Leibowitz et al., 2014; Sawicz et al., 2011; Wigington et al., 2013). The appropriate choice of clusters for the k-means method is less unambiguous (Ketchen and Shook, 1996). The change in number of clusters when the sum of squared distances to our cluster centres only reduces marginally was not clearly definable (~~Figure A 1~~~~Figure A-1~~). However, choosing only 3 clusters instead of 4 would have resulted in unrealistic spatial distribution of clusters. The attribution of Northern African regions with Northern Europe to the same cluster occurred because of their similarity of altitude ranges (~~Table 4~~~~Table 4~~). On the other hand, a selection of 5 clusters would have resulted in a cluster with properties just between the MTN and the MED clusters and, because of a much stronger scattering, weaker spatial distinction between them. With 4 clusters our karst landscapes are similar to the Koeppen Geiger climate regions (Kottek et al., 2006), in particular the Oceanic Climate (HUM), the Hot and Warm summer Mediterranean Climate (MED), and the Hot Desert Climates (DES). We see deviations when comparing the Polar and Alpine Climate regions of Koeppen-Geiger with our High Range Mountain karst landscape though, since our landscapes are also defined by their elevation ranges.

The borders of these hydrologic landscapes are also uncertain. Natural systems usually do not have ~~as~~-straight borders that fall on a grid as assumed by this analysis. Typical ~~T~~transitions between landscape types are ~~rather~~-continuous and hence transitions from a parameter set representing one landscape to another parameter set of another cluster should be ~~transient~~graded, as well. This will be discussed in the following subsection.

4.1.2 Confinement of parameters

How the 3 steps of the parameter confinement strategy reduce the initial sample shows which type of data provides the most relevant information for each of the karst landscapes. While the timing of actual evapotranspiration and soil saturation that is expressed by the correlation rule appears to be most relevant for the humid landscapes, the bias rule, which represents the volumes of monthly evapotranspiration is more relevant for the mountain and Mediterranean landscapes. Swapping the order of the correlation rule and the bias rule ~~in their order~~ would

provide the same results for HUM and MTN. But for MED the ~~other~~-alternative order increases the importance of timing expressed by the correlation rule indicating the similar importance of both confinement steps.

The thresholds we set in confinement step 1 and 2 are not very strict, and the ranges of soil storage capacity we used as *a priori* information in step 3 are quite large. This compensates for the fact that (1) only recharge-related variables are available rather than direct recharge observations, (2) these variables are not available at the simulation scale (0.25° grid) but at a point-scale, and (3) the transition between the landscapes is more continuous than discrete. Despite these rather weak constraints, the initial parameter sample of 25,000 reduces to a quite low number between 679 (HUM) and 2,731 (MED). All *posterior* parameters overlap except for the soil storage capacities that are tailored by the *a priori* information (confinement step 3). Hence, a little number of parameter sets for one landscape is also acceptable for some of the other landscape and therefore taking into account the continuous transition between them.

All model parameters, except for V_{epi} , show different shapes in their cumulative distribution functions across the karst landscapes. The desert landscape parameters only differ from the initial sample for the V_{soil} parameter due to the lack of information to apply confinement steps 1 and 2. The distribution parameter a is found at the lower values of its feasible range for the humid and mountain landscapes indicating a significant contribution of preferential recharge. Since altitude ranges are rather low for HUM this may be attributed to a significant epikarst development (Perrin et al., 2003; Williams, 1983). For MTN a mixture of epikarst development and topography driven interflow at the mountain hill slopes and valleys can be expected to control the dynamics of karstic recharge (Scanlon et al., 2002; Tague and Grant, 2009). At the Mediterranean landscapes the a parameter adapts to ranges that are rather found at the higher values of its initial range indicating that there is a stronger differentiation between diffuse and concentrated recharge. This may be due to the generally thinner soils (Table 5~~Table 5~~) that limit the availability of CO₂ for karst evolution (Ford and Williams, 2007). Instead, local surface runoff channels the water to the next enlarged fissure or crack to reach the subsurface as concentrated recharge (Lange et al., 2003). The epikarst storage coefficient K_{epi} for HUM and MED is at lower values of the initial range indicating realistic mean residence times of days to weeks (Aquilina et al., 2006; Hartmann et al., 2013a). The MTN landscapes show larger K_{epi} values indicating slower epikarst dynamics most probably

due to the reasons mentioned above. The application of *a priori* information in confinement step 3 automatically tailors the values of V_{soil} to ranges that we assume to be realistic. The fact that confinement steps 1 and 2 already push the shape of their *posteriors* towards the *a priori* ranges corroborates that assumption.

The little changes that occur to the initial distributions of the DES parameter sets elaborate the flexibility of our parameter assessment strategy. The *posterior* distribution evolves only where information is available (for this landscape on V_{soil}). This is also evident in the behaviour of parameter V_{epi} . The available information is just not precise enough to achieve identification beyond its *a priori* ranges. For parameter a in HUM, MTN and MED, a lot of information is derived from the available data and its *posteriors* differ strongly from its initial distribution, while there is less information to determine K_{epi} . This explicit handling of uncertainties in the parameter identification process allows us to provide recharge simulations over Europe's karst regions with uncertainty estimates that represent confidence for each of the identified karst landscapes.

4.2 Simulation of karst recharge over Europe and the Mediterranean

4.2.1 Realism of spatial patterns

Simulated mean annual recharge ~~volumes~~ amounts for the period 2002/03-2011/12 show a wide range of values, from 0 >1000 mm/a (Figure 7~~Figure 7~~). Total water availability (mean annual precipitation) appears to be the main driver for its spatial pattern in many regions, for instance at former Yugoslavia or Northern UK. This is consistent with findings of other studies (Hartmann et al., 2014c; Samuels et al., 2010). When we normalize the recharge rates by the observed precipitation amounts we find that water availability is not the only control on mean annual recharge volumes. A strong relation of evapotranspiration and karst characteristics and processes was shown in many studies and is also found here (Heilman et al., 2014; Jukic and Denic-Jukic, 2008). Potential evaporation is generally increasing from North to South and has an important impact on recharge rates as well; for instance on the Arabian Peninsula or in the Alps.

Mountain ranges are considered to be the water towers of the world (Viviroli et al., 2007). Here the MTN landscapes also show the largest recharge volumes due to the large precipitation volumes they receive, though with a considerable spread in our study. HUM and MED landscapes behave similarly with significantly less recharge than MTN. Not

surprisingly there is not much recharge in the desert landscapes at all. But the differences among the clusters shift when considering recharge rates. Due to their thin soils, and therefore low soil storage for evaporation (Table 5Table-5), the DES karst landscapes transfer up to 45% of the little precipitation they receive into recharge. The MED landscapes show similarly high recharge rates. Though since their soils are generally thicker than the DES soils the typical seasonal and convective rainfall patterns of the Mediterranean climate (Goldreich, 2003; Lionello, 2012) might have an important impact, too.

Even though there is still considerable spread in our confined parameter sets, the uncertainty in simulated mean annual recharge volumes is quite low. The uncertainties that follow the limited information ~~content of the~~contained in the observations are revealed more clearly when we relate the standard deviation of simulated recharge to its mean volumes with the coefficient of variation. The uncertainty for the DES landscape is the largest among the clusters because *a priori* information is only available for V_{soil} . The uncertainty reduces for the MED and MTN landscapes. The low uncertainties for the coefficient of variation of our recharge simulations for the HUM landscape indicate that the available data contained significant information for confining the model parameter ranges.

4.2.2 Relevance of different recharge processes to simulation time scales

The mean annual water balance of a hydrological system is dominated by the separation of precipitation into actual evapotranspiration and discharge (Budyko and Miller, 1974; Sivapalan et al., 2011). Actual evapotranspiration is controlled by the soil storage capacity V_{soil} and the distribution coefficient a within the VarKarst-R model. Regional sensitivity analysis shows that both of them are most sensitive for the 10-year and annual time scale (Figure 10Figure-10). Both parameters loose some impact at higher temporal resolutions (seasonal or monthly time scale) in favour of the parameters that control the dynamics of the epikarst. This behaviour is consistent with evidence from field and other modelling studies that showed that the epikarst can be considered as a temporary storage and distribution system for karstic recharge (Hartmann et al., 2012; Williams, 1983) – potentially storing water for several days to weeks (Aquilina et al., 2006; Hartmann et al., 2013a). Parameter V_{epi} does not show much sensitivity across all landscapes as suggested by the *posterior* distributions of the confinement strategy. First of all, this finding indicates that the data we used for our confinement strategy do not bias the general model behaviour. It also shows that for the

epikarst storage and flow dynamics K_{epi} is much more important when simulating at monthly or seasonal resolution.

Furthermore, the results of the regional sensitivity analysis show which parameters are most important at a given time scale. Depending on the purpose a new study may start with the initial ranges of the model parameters or it might continue with the confined parameter ranges that we found here. The latter would result in slightly different sensitivities (Figure A 2Figure A-2). For both cases, the epikarst parameters will require more attention when applying the VarKarst-R model for simulations at seasonal or monthly time scales. When working at a smaller spatial scale, ~~additional-combined~~ analysis of spring discharge and its hydrochemistry may provide such additional information (Lee and Krothe, 2001; Mudarra and Andreo, 2011). When working at a time scale of >1 year the ~~distribution-parameter-variability constant~~ a and the soil storage capacity V_{soil} require most attention if one starts from the initial ranges. The distribution parameter is most important when using the confined ranges. Again, spring discharge analysis may help to understand the degree of karstification (Király, 2003) and the distribution of concentrated and diffuse recharge mechanisms that are controlled by a . In addition, more precise digital elevation models or soil maps may help to better identify a and V_{soil} . A limitation of the regional sensitivity analysis approach used here is that parameter interactions are only included implicitly, considering parameter interactions with more elaborated methods (Saltelli et al., 2008) may reveal even more characteristics of the VarKarst-R model at different simulation time scales. But this is beyond the scope of this ~~study~~paper.

4.3 Impact of karstic subsurface heterogeneity

Even though some deviations occur among the individual karst landscapes, the general simulations of the VarKarst-R model follow ~~well the~~ observations of mean annual recharge rates over Europe ~~and the Mediterranean well~~ (Figure 9Figure-9). On the other hand, the widely-used large-scale simulation models PCR-GLOBWB (Wada et al., 2010, 2014) and WaterGAP (Döll and Fiedler, 2008b; Döll et al., 2003) generally under-estimate groundwater recharge (Table 6Table-6). The reason for this is the representation of karstic subsurface heterogeneity within the VarKarst-R model, i.e. the inclusion of preferential flowpaths and of subsurface heterogeneity. Based on the conceptual understanding of soil and epikarst storage behaviour (Figure 1Figure-1c) it allows (1) for more recharge during wet conditions because surface runoff ~~does not exist~~is not generated, and (2) for more recharge during dry conditions

because the thin soil compartments will always allow for some water to percolate downwards before it is consumed by evapotranspiration. During wet conditions, both PCR-GLOBWB and WaterGAP would produce surface runoff instead that is ~~therefore-subsequently~~ lost from groundwater recharge. During dry conditions, due to its non-variable soil storage capacity, the PCR-GLOBWB model would not produce any recharge when the soil water is below its minimum storage. Separating surface runoff and groundwater recharge by a constant factor the WaterGAP model would produce recharge during dry conditions, but a constant fraction of effective precipitation will always become fast surface/subsurface runoff resulting in reduced recharge volumes.

This does not mean that the representation of recharge processes in models like PCR-GLOBWB or WaterGAP is generally wrong, but can be limited since our analysis shows that the structures of such models need more adaption to the particularities of different hydrologic landscapes. In particular it adds to the need for incorporating sub-grid heterogeneity in our large-scale simulation models (Beven and Cloke, 2012). Karst regions ~~contribute-comprise~~ about 35% of Europe's land surface and our results indicate that presently their groundwater recharge is under-estimated, while surface runoff and actual evaporation are over-estimated. Given the expected decrease of precipitation in semi-arid regions, such as the Mediterranean, and an increase of extreme rainfall events at the same time in the near future (2016-2035, Kirtman et al., 2013) ~~present-current~~ large-scale simulation models will over-estimate both the vulnerability of groundwater recharge and the flood hazard in ~~Europe's~~ karst regions in Europe and the Mediterranean. The same is true for the long-term future (end of 21st century, Collins et al., 2013). Of course, an over-estimation of vulnerability and hazard might be the "lesser evil" compared to an over-estimation. But at times of limited financial resources excessive investments ~~in ensuring the security of drinking water supply into drinking water~~ and flood risk management for potential future changes may unnecessarily aggravate the socio-economic impacts of climate change.

5 Conclusions

In this study we have presented the first attempt to model groundwater recharge over all karst regions in Europe and the Mediterranean. The model application was made possible by a novel parameter confinement strategy that utilized a combination of *a priori* information and recharge related observations on 4 typical karst landscapes that were identified through cluster analysis. Handling the remaining uncertainty explicitly as *posterior* parameter distributions

564 resulting from the confinement strategy we were finally able to produce recharge simulations
565 and an estimate of their uncertainty ~~over Europe's karst regions~~. We found an adequate
566 agreement with our new model when comparing our results with independent observations of
567 recharge at study sites over Europe and the Mediterranean. We further show that ~~present~~
568 current large-scale modelling approaches tend to significantly under-estimate recharge
569 volumes.

570 Overall, our analysis showed that the subsurface heterogeneity of karst regions and the
571 presence of preferential flowpaths enhances recharge. It results in high infiltration capacities
572 prohibiting surface runoff and reducing actual evapotranspiration during wet conditions. On
573 the other hand it allows for recharge during dry conditions because some water can always
574 percolate downwards passing the thin fraction of the distributed soil depths. This particular
575 behaviour suggests that karstic regions might be more resilient to climate change in terms of
576 both flooding and droughts. Drinking water and flood risk management is ~~prone-labile~~ to be
577 based on erroneous information at least at the 35% of Europe's land surface since this is not
578 considered in current large-scale modelling approaches.

579 However, using recharge directly as a proxy for "available" groundwater resources may not
580 be good in all cases, neither in karst regions nor in other types of aquifers (Bredehoeft, 2002).
581 To precisely estimate the sustainably usable fraction of groundwater the aquifer outflow
582 should be known rather than just the inflow. Further pumping~~than the inflow and pumping~~
583 strategies should consider the geometry and transmissivity of the aquifer. Hence, recharge
584 estimation can be considered only as a first proxy of available groundwater and future studies
585 should focus on the large-scale simulation of karst groundwater flow and storage to further
586 improve water resources predictions in karst regions.

587 **Acknowledgements**

588 We want to thank Juergen Strub, research associate ~~from~~at the Chair of Hydrology, Freiburg,
589 Germany, for designing some of the figures and Thomas Godman for collecting references to
590 independent recharge studies. This work was supported by a fellowship within the Postdoc
591 Programme of the German Academic Exchange Service [Andreas Hartmann, DAAD] and by
592 the UK Natural Environment Research Council [Francesca Pianosi, CREDIBLE Project;
593 grant number NE/J017450/1]. The sensitivity analysis was carried out by the SAFE Toolbox
594 (<http://bristol.ac.uk/cabot/resources/safe-toolbox/>). We thank Petra Döll for providing the

mean annual recharge volumes of WaterGAP, and Fanny Sarazin for checking the results of the regional sensitivity analysis.

References

Allocca, V., Manna, F. and De Vita, P.: Estimating annual groundwater recharge coefficient for karst aquifers of the southern Apennines (Italy), *Hydrol. Earth Syst. Sci.*, 18(2), 803–817, doi:10.5194/hess-18-803-2014, 2014.

Andreo, B., Vías, J., Durán, J., Jiménez, P., López-Geta, J. and Carrasco, F.: Methodology for groundwater recharge assessment in carbonate aquifers: application to pilot sites in southern Spain, *Hydrogeol. J.*, 16(5), 911–925 [online] Available from: <http://dx.doi.org/10.1007/s10040-008-0274-5>, 2008.

Aquilina, L., Ladouche, B. and Doerfliger, N.: Water storage and transfer in the epikarst of karstic systems during high flow periods, *J. Hydrol.*, 327, 472–485, 2006.

Arnell, N. W.: Relative effects of multi-decadal climatic variability and changes in the mean and variability of climate due to global warming : future streamflows in Britain, *J. Hydrol.*, 270, 195–213, 2003.

Aydin, H., Ekmekci, M. and Soylu, M. E.: Characterization and conceptualization of a relict karst aquifer (bilecik , turkey) karakterizacija in konceptualizacija reliktnege, *Acta carsologica*, 42(1), 75–92, 2013.

Bakalowicz, M.: Karst groundwater: a challenge for new resources, *Hydrogeol. J.*, 13, 148–160, 2005.

Bakalowicz, M., El, Æ. M. and El-hajj, A.: Karst groundwater resources in the countries of eastern Mediterranean : the example of Lebanon, *Environ. Geol.*, 54, 597–604, doi:10.1007/s00254-007-0854-z, 2008.

Baldocchi, D., Falge, E., Gu, L., Olson, R., Hollinger, D., Running, S., Anthoni, P., Bernhofer, C., Davis, K., Evans, R., Fuentes, J., Goldstein, A., Katul, G., Law, B., Lee, X., Malhi, Y., Meyers, T., Munger, W., Oechel, W., Paw, K. T., Pilegaard, K., Schmid, H. P., Valentini, R., Verma, S., Vesala, T., Wilson, K. and Wofsy, S.: FLUXNET: A New Tool to Study the Temporal and Spatial Variability of Ecosystem–Scale Carbon Dioxide, Water Vapor, and Energy Flux Densities, *Bull. Am. Meteorol. Soc.*, 82(11), 2415–2434, doi:10.1175/1520-0477(2001)082<2415:fantts>2.3.co;2, 2001.

Barbieri, M., Boschetti, T., Petitta, M. and Tallini, M.: Stable isotope (2H , 18O and $87\text{Sr}/86\text{Sr}$) and hydrochemistry monitoring for groundwater hydrodynamics analysis in a karst aquifer (Gran Sasso, Central Italy), *Appl. Geochemistry*, 20(11), 2063–2081, doi:10.1016/j.apgeochem.2005.07.008, 2005.

630 Beven, K. J. and Cloke, H. L.: Comment on “Hyperresolution global land surface modeling:
 631 Meeting a grand challenge for monitoring Earth’s terrestrial water” by Eric F. Wood et al.,
 632 Water Resour. Res., 48(1), W01801, doi:10.1029/2011WR010982, 2012.

633 Bonacci, O.: Analysis of the maximum discharge of karst springs, Hydrogeol. J., 9(4), 328–
 634 338, doi:10.1007/s100400100142, 2001.

635 Bredehoeft, J. D.: The water budget myth revisited: why hydrogeologists model, Ground
 636 Water, 40(4), 340–345, 2002.

637 Budyko, D. H. and Miller, M. I.: Climate and life, Academic press, New York., 1974.

638 Butscher, C. and Huggenberger, P.: Intrinsic vulnerability assessment in karst areas: A
 639 numerical modeling approach, Water Resour. Res., 44, W03408,
 640 doi:10.1029/2007WR006277, 2008.

641 Christensen, J. H., Hewitson, B., Busuioc, A., Chen, A., Gao, X., Held, I., Jones, R., Kolli, R.
 642 K., Kwon, W.-T., Laprise, R., Rueda, V. M., Mearns, L., Menéndez, C. G., Räisänen, J.,
 643 Rinke, A., Sarr, A. and Whetton, P.: Regional Climate Projections, in Climate Change 2007:
 644 The Physical Science Basis. Contribution of Working Group I to the Fourth Assessment
 645 Report of the Intergovernmental Panel on Climate Change, edited by S. Solomon, D. Qin, M.
 646 Manning, Z. Chen, M. Marquis, K. B. Averyt, M. Tignor, and H. L. Miller, p. 996,
 647 Cambridge University Press, Cambridge, United Kingdom and New York, NY, USA. [online]
 648 Available from:
 649 [http://www.ipcc.ch/publications_and_data/publications_ipcc_fourth_assessment_report_wg1_](http://www.ipcc.ch/publications_and_data/publications_ipcc_fourth_assessment_report_wg1_report_the_physical_science_basis.htm)
 650 [report_the_physical_science_basis.htm](http://www.ipcc.ch/publications_and_data/publications_ipcc_fourth_assessment_report_wg1_report_the_physical_science_basis.htm), 2007.

651 Collins, M., Knutti, R., Arblaster, J. M., Dufresne, J.-L., Fichefet, T., Friedlingstein, P., Gao,
 652 X., Gutowski, W. J., Johns, T. and Krinner, G.: Long-term climate change: projections,
 653 commitments and irreversibility, in Climate Change 2013: The Physical Science Basis.
 654 Contribution of Working Group I to the Fifth Assessment Report of the Intergovernmental
 655 Panel on Climate Change, edited by T. F. Stocker, D. Qin, G.-K. Plattner, M. Tignor, S. K.
 656 Allen, J. Boschung, A. Nauels, Y. Xia, V. Bex, and P. M. Midgley, pp. 1029–1136,
 657 Cambridge University Press, Cambridge, United Kingdom and New York, NY, USA., 2013.

658 COST: COST 65: Hydrogeological aspects of groundwater protection in karstic areas, Final
 659 report (COST action 65), edited by D.-G. X. I. I. S. European Comission Research and
 660 Development, Eur. Comm. Dir. XII Sci. Res. Dev., Report EUR, 446, 1995.

661 Dai, A.: Increasing drought under global warming in observations and models, Nat. Clim.
 662 Chang., 3(1), 52–58, doi:10.1038/nclimate1633, 2012.

663 Döll, P. and Fiedler, K.: Global-scale modeling of groundwater recharge, Hydrol. Earth Syst.
 664 Sci., 12(3), 863–885, doi:10.5194/hess-12-863-2008, 2008a.

665 Döll, P. and Fiedler, K.: Global-scale modeling of groundwater recharge, Hydrol. Earth Syst.
 666 Sci., 12(3), 863–885, doi:10.5194/hess-12-863-2008, 2008b.

667 Döll, P., Kaspar, F. and Lehner, B.: A global hydrological model for deriving water
668 availability indicators: model tuning and validation, *J. Hydrol.*, 270(1-2), 105–134,
669 doi:10.1016/S0022-1694(02)00283-4, 2003.

670 Dorigo, W. A., Wagner, W., Hohensinn, R., Hahn, S., Paulik, C., Xaver, A., Gruber, A.,
671 Drusch, M., Mecklenburg, S., van Oevelen, P., Robock, A. and Jackson, T.: The International
672 Soil Moisture Network: a data hosting facility for global in situ soil moisture measurements,
673 *Hydrol. Earth Syst. Sci.*, 15(5), 1675–1698, doi:10.5194/hess-15-1675-2011, 2011.

674 Doummar, J., Sauter, M. and Geyer, T.: Simulation of flow processes in a large scale karst
675 system with an integrated catchment model (Mike She) – Identification of relevant parameters
676 influencing spring discharge, *J. Hydrol.*, 426-427, 112–123,
677 doi:10.1016/j.jhydrol.2012.01.021, 2012.

678 Einsiedl, F.: Flow system dynamics and water storage of a fissured-porous karst aquifer
679 characterized by artificial and environmental tracers, *J. Hydrol.*, 312, 312–321, 2005.

680 Ek, M. B.: Implementation of Noah land surface model advances in the National Centers for
681 Environmental Prediction operational mesoscale Eta model, *J. Geophys. Res.*, 108(D22),
682 doi:10.1029/2002jd003296, 2003.

683 FAO/IIASA/ISRIC/ISSCAS/JRCv: Harmonized World Soil Database (version 1.2), edited by
684 FAO/IIASA, 2012.

685 Fleury, P., Plagnes, V. and Bakalowicz, M.: Modelling of the functioning of karst aquifers
686 with a reservoir model: Application to Fontaine de Vaucluse (South of France), *J. Hydrol.*,
687 345, 38–49, 2007.

688 Ford, D. C. and Williams, P. W.: *Karst Hydrogeology and Geomorphology*, Wiley,
689 Chichester., 2007.

690 Foster, S. S. D.: Groundwater recharge and pollution vulnerability of British aquifers: a
691 critical overview, *Geol. Soc. London, Spec. Publ.*, 130, 7–22,
692 doi:10.1144/GSL.SP.1998.130.01.02, 1998.

693 Gleeson, T., Moosdorf, N., Hartmann, J. and van Beek, L. P. H.: A glimpse beneath earth's
694 surface: GLobal HYdrogeology MaPS (GLHYMPS) of permeability and porosity, *Geophys.*
695 *Res. Lett.*, n/a–n/a, doi:10.1002/2014gl059856, 2014a.

696 Gleeson, T., Moosdorf, N., Hartmann, J. and van Beek, L. P. H.: A glimpse beneath earth's
697 surface: GLobal HYdrogeology MaPS (GLHYMPS) of permeability and porosity, *Geophys.*
698 *Res. Lett.*, 41(11), 3891–3898, doi:10.1002/2014GL059856, 2014b.

699 Gleeson, T., Wada, Y., Bierkens, M. F. and van Beek, L. P.: Water balance of global aquifers
700 revealed by groundwater footprint, *Nature*, 488(7410), 197–200, doi:10.1038/nature11295,
701 2012.

702 Goldreich, Y.: *The climate of Israel: observation, research and application*, Kluwer
703 Academic/Plenum Publishers., 2003.

704 GRDC: Long Term Mean Annual Freshwater Surface Water Fluxes into the World Oceans,
 705 Comparisons of GRDC freshwater flux estimate with literature. [online] Available from:
 706 <http://grdc.bafg.de/servlet/is/7083/>, 2004.

707 Hartmann, A., Barberá, J. A., Lange, J., Andreo, B. and Weiler, M.: Progress in the
 708 hydrologic simulation of time variant recharge areas of karst systems – Exemplified at a karst
 709 spring in Southern Spain, *Adv. Water Resour.*, 54, 149–160,
 710 doi:10.1016/j.advwatres.2013.01.010, 2013a.

711 Hartmann, A., Goldscheider, N., Wagener, T., Lange, J. and Weiler, M.: Karst water
 712 resources in a changing world: Review of hydrological modeling approaches, *Rev. Geophys.*,
 713 DOI: 10.1002/2013rg000443, doi:10.1002/2013rg000443, 2014a.

714 Hartmann, A., Kobler, J., Kralik, M., Dirnböck, T., Humer, F. and Weiler, M.: Transit time
 715 distributions to understand the biogeochemical impacts of storm Kyrill on an Austrian karst
 716 system, *Biogeosciences*, submitted, 2015.

717 Hartmann, A., Lange, J., Weiler, M., Arbel, Y. and Greenbaum, N.: A new approach to model
 718 the spatial and temporal variability of recharge to karst aquifers, *Hydrol. Earth Syst. Sci.*,
 719 16(7), 2219–2231, doi:10.5194/hess-16-2219-2012, 2012.

720 Hartmann, A., Mudarra, M., Andreo, B., Marin, A., Wagener, T. and Lange, J.: Modeling
 721 spatio-temporal impacts of hydro-climatic extremes on a karst aquifer in Southern Spain,
 722 *Water Resour. Res.*, moderate revisions, resubmit until July 2014,
 723 doi:10.1002/2014WR015685, 2014b.

724 Hartmann, A., Mudarra, M., Andreo, B., Marín, A., Wagener, T. and Lange, J.: Modeling
 725 spatiotemporal impacts of hydroclimatic extremes on groundwater recharge at a
 726 Mediterranean karst aquifer, *Water Resour. Res.*, n/a–n/a, doi:10.1002/2014WR015685,
 727 2014c.

728 Hartmann, A., Weiler, M., Wagener, T., Lange, J., Kralik, M., Humer, F., Mizyed, N.,
 729 Rimmer, A., Barberá, J. A., Andreo, B., Butscher, C. and Huggenberger, P.: Process-based
 730 karst modelling to relate hydrodynamic and hydrochemical characteristics to system
 731 properties, *Hydrol. Earth Syst. Sci.*, 17(8), 3305–3321, doi:10.5194/hess-17-3305-2013,
 732 2013b.

733 Hatipoglu-Bagci, Z. and Sazan, M. S.: Characteristics of karst springs in Aydıncık (Mersin ,
 734 Turkey), based on recession curves and hydrochemical and isotopic parameters, *Q. J. Eng.*
 735 *Geol. Hydrogeol.*, 47(1), 89–99, 2014.

736 Heilman, J. L., Litvak, M. E., McInnes, K. J., Kjølgaard, J. F., Kamps, R. H. and Schwinning,
 737 S.: Water-storage capacity controls energy partitioning and water use in karst ecosystems on
 738 the Edwards Plateau, Texas, *Ecohydrology*, 7(1), 127–138, doi:10.1002/eco.1327, 2014.

739 Hirabayashi, Y., Mahendran, R., Koirala, S., Konoshima, L., Yamazaki, D., Watanabe, S.,
 740 Kim, H. and Kanae, S.: Global flood risk under climate change, *Nat. Clim. Chang.*, 3(9), 816–
 741 821, doi:10.1038/nclimate1911, 2013.

- 742 Hoetzi, H.: Groundwater recharge in an arid karst area (Saudi Arabia), IAHS Publ.
743 (International Assoc. Hydrol. Sci., 232, 195–207, 1995.
- 744 Hughes, A. G., Mansour, M. M. and Robins, N. S.: Evaluation of distributed recharge in an
745 upland semi-arid karst system: the West Bank Mountain Aquifer, Middle East, *Hydrogeol. J.*,
746 16, 845–854, 2008.
- 747 Jackson, C. R., Meister, R. and Prudhomme, C.: Modelling the effects of climate change and
748 its uncertainty on UK Chalk groundwater resources from an ensemble of global climate
749 model projections, *J. Hydrol.*, In Press, doi:10.1016/j.jhydrol.2010.12.028, 2010.
- 750 Jeannin, P.-Y. and Grasso, D. A.: Permeability and hydrodynamic behavior of karstic
751 environment, in *Karst Waters Environmental Impact*, edited by G. Gunay and A. I. Johnson,
752 pp. 335–342, A.A. Balkema, Rotterdam., 1997.
- 753 Jukic, D. and Denic-Jukic, V.: Estimating parameters of groundwater recharge model in
754 frequency domain: Karst springs Jadro and Žrnovnica, *Hydrol. Process.*, 22, 4532–4542,
755 2008.
- 756 Ketchen, D. J. and Shook, C. L.: The application of cluster analysis, *Strateg. Manag. J.*,
757 17(November 1994), 441–458, 1996.
- 758 Kiraly, L.: Modelling karst aquifers by the combined discrete channel and continuum
759 approach, *Bull. d’Hydrogéologie*, 16, 77–98, 1998.
- 760 Kiraly, L.: Karstification and Groundwater Flow, *Speleogenes. Evol. Karst Aquifers*, 1(3), 1–
761 24, 2003.
- 762 Kirtman, B., Power, S. B., Adedoyin, J. A., Boer, G. J., Bojariu, R., Camilloni, I., Doblas-
763 Reyes, F. J., Fiore, A. M., Kimoto, M. and Meehl, G. A.: Near-term climate change:
764 projections and predictability, in *Climate Change 2013: The Physical Science Basis*.
765 Contribution of Working Group I to the Fifth Assessment Report of the Intergovernmental
766 Panel on Climate Change, edited by T. F. Stocker, D. Qin, G.-K. Plattner, M. Tignor, S. K.
767 Allen, J. Boschung, A. Nauels, Y. Xia, V. Bex, and P. M. Midgley, pp. 953–1028, Cambridge
768 University Press, Cambridge, United Kingdom and New York, NY, USA., 2013.
- 769 Kotteck, M., Grieser, J., Beck, C., Rudolf, B. and Rubel, F.: World Map of the Köppen-Geiger
770 climate classification updated, *Meteorol. Zeitschrift*, 15(3), 259–263, doi:10.1127/0941-
771 2948/2006/0130, 2006.
- 772 Koutroulis, A. G., Tsanis, I. K., Daliakopoulos, I. N. and Jacob, D.: Impact of climate change
773 on water resources status: A case study for Crete Island, Greece, *J. Hydrol.*, 479, 146–158,
774 doi:10.1016/j.jhydrol.2012.11.055, 2013.
- 775 Lange, J., Greenbaum, N., Husary, S., Ghanem, M., Leibundgut, C. and Schick, A. P.: Runoff
776 generation from successive simulated rainfalls on a rocky, semi-arid, Mediterranean hillslope,
777 *Hydrol. Process.*, 17(2), 279–296, doi:10.1002/hyp.1124, 2003.

778 Lee, E. S. and Krothe, N. C.: A four-component mixing model for water in a karst terrain in
 779 south-central Indiana, USA. Using solute concentration and stable isotopes as tracers, *Chem.*
 780 *Geol.*, 179, 2001.

781 Leibowitz, S. G., Comeleo, R. L., Wigington Jr., P. J., Weaver, C. P., Morefield, P. E.,
 782 Sproles, E. a. and Ebersole, J. L.: Hydrologic landscape classification evaluates streamflow
 783 vulnerability to climate change in Oregon, USA, *Hydrol. Earth Syst. Sci.*, 18(9), 3367–3392,
 784 doi:10.5194/hess-18-3367-2014, 2014.

785 Lerner, D. N., Issar, A. S. and Simmers, I.: Groundwater recharge : a guide to understanding
 786 and estimating natural recharge, Heise, Hannover., 1990.

787 Lionello, P.: The Climate of the Mediterranean Region: From the past to the future, Elsevier.,
 788 2012.

789 Maloszewski, P., Stichler, W., Zuber, A. and Rank, D.: Identifying the flow systems in a
 790 karstic-fissured-porous aquifer, the Schneealpe, Austria, by modelling of environmental ^{18}O
 791 and ^3H isotopes, *J. Hydrol.*, 256, 48–59, 2002.

792 Milly, P. C. D., Dunne, K. A. and Vecchia, A. V: Global pattern of trends in streamflow and
 793 water availability in a changing climate, *Nature*, 438(7066), 347–350,
 794 doi:10.1038/nature04312, 2005.

795 Miralles, D. G., Holmes, T. R. H., De Jeu, R. A. M., Gash, J. H., Meesters, A. G. C. A. and
 796 Dolman, A. J.: Global land-surface evaporation estimated from satellite-based observations,
 797 *Hydrol. Earth Syst. Sci.*, 15(2), 453–469, doi:10.5194/hess-15-453-2011, 2011.

798 Le Moine, N., Andréassian, V. and Mathevet, T.: Confronting surface- and groundwater
 799 balances on the La Rochefoucauld-Touvre karstic system (Charente, France), *Water Resour.*
 800 *Res.*, 44, W03403, doi:10.1029/2007WR005984, 2008.

801 Le Moine, N., Andréassian, V., Perrin, C. and Michel, C.: How can rainfall-runoff models
 802 handle intercatchment groundwater flows? Theoretical study based on 1040 French
 803 catchments, *Water Resour. Res.*, 43, W06428, doi:10.1029/2006WR005608, 2007.

804 Mudarra, M. and Andreo, B.: Relative importance of the saturated and the unsaturated zones
 805 in the hydrogeological functioning of karst aquifers: The case of Alta Cadena (Southern
 806 Spain), *J. Hydrol.*, 397(3-4), 263–280, doi:10.1016/j.jhydrol.2010.12.005, 2011.

807 Padilla, A., Pulido-Bosch, A. and Mangin, A.: Relative Importance of Baseflow and
 808 Quickflow from Hydrographs of Karst Spring, *Ground Water*, 32(2), 267–277, 1994.

809 Perrin, J., Jeannin, P.-Y. and Zwahlen, F.: Epikarst storage in a karst aquifer: a conceptual
 810 model based on isotopic data, Milandre test site, Switzerland, *J. Hydrol.*, 279, 106–124, 2003.

811 Priestley, C. H. B. and Taylor, R. J.: On the Assessment of Surface Heat Flux and
 812 Evaporation Using Large-Scale Parameters, *Mon. Weather Rev.*, 100(2), 81–92,
 813 doi:10.1175/1520-0493(1972)100<0081:OTAOSH>2.3.CO;2, 1972.

814 Quinn, J. J., Tomasko, D. and Kuiper, J. A.: Modeling complex flow in a karst aquifer,
815 Sediment. Geol., 184, 343–352, 2006.

816 Rimmer, A. and Hartmann, A.: Simplified conceptual structures and analytical solutions for
817 groundwater discharge using reservoir equations, Water Resour. Manag. Model. Ed. by DPC
818 Nayak, InTech, Kakinada, India, 217–338, 2012.

819 Rodell, M., Houser, P. R., Jambor, U., Gottschalck, J., Mitchell, K., Meng, C.-J., Arsenault,
820 K., Cosgrove, B., Radakovich, J., Bosilovich, M., Entin, J. K., Walker, J. P., Lohmann, D. and
821 Toll, D.: The Global Land Data Assimilation System, Bull. Am. Meteorol. Soc., 85(3), 381–
822 394, doi:10.1175/BAMS-85-3-381, 2004.

823 Rui, H. and Beaudoin, H.: README Document for Global Land Data Assimilation System
824 Version 2 (GLDAS-2) Products, GES DISC / HSL [online] Available from:
825 <http://hydro1.sci.gsfc.nasa.gov/data/s4pa/GLDAS/README.GLDAS2.pdf>, 2013.

826 Saltelli, A., Ratto, M., Andres, T., Campolongo, F., Cariboni, J., Gatelli, D., Saisana, M. and
827 Tarantola, S.: Global sensitivity analysis: the primer, John Wiley & Sons., 2008.

828 Samuels, R., Rimmer, A., Hartmann, A., Krichak, S. and Alpert, P.: Climate Change Impacts
829 on Jordan River Flow: Downscaling Application from a Regional Climate Model, J.
830 Hydrometeorol., 11(4), 860–879, doi:DOI 10.1175/2010JHM1177.1, 2010.

831 Sawicz, K., Wagener, T., Sivapalan, M., Troch, P. A. and Carrillo, G.: Catchment
832 classification: empirical analysis of hydrologic similarity based on catchment function in the
833 eastern USA, Hydrol. Earth Syst. Sci., 15(9), 2895–2911, doi:10.5194/hess-15-2895-2011,
834 2011.

835 Scanlon, B., Healy, R. and Cook, P.: Choosing appropriate techniques for quantifying
836 groundwater recharge, Hydrogeol. J., 10(1), 18–39 [online] Available from:
837 <http://dx.doi.org/10.1007/s10040-001-0176-2>, 2002.

838 Seber, G. A. F.: Multivariate observations, John Wiley & Sons., 2009.

839 Sivapalan, M., Yaeger, M. a., Harman, C. J., Xu, X. and Troch, P. a.: Functional model of
840 water balance variability at the catchment scale: 1. Evidence of hydrologic similarity and
841 space-time symmetry, Water Resour. Res., 47(2), W02522, doi:10.1029/2010WR009568,
842 2011.

843 Spear, R. C. and Hornberger, G. M.: Eutrophication in peel inlet - II. Identification of critical
844 uncertainties via generalized sensitivity analysis, Water Resour. Res., 14, 43–49, 1980.

845 Tague, C. and Grant, G. E.: Groundwater dynamics mediate low-flow response to global
846 warming in snow-dominated alpine regions, Water Resour. Res., 45(7), W07421,
847 doi:10.1029/2008WR007179, 2009.

848 Tritz, S., Guinot, V. and Jourde, H.: Modelling the behaviour of a karst system catchment
849 using non-linear hysteretic conceptual model, J. Hydrol., 397(3-4), 250–262,
850 doi:10.1016/j.jhydrol.2010.12.001, 2011.

851 USGS: Shuttle Radar Topography Mission, 3 Arc Second scene SRTM V2.1, edited by U. of
852 M. Global Land Cover Facility, 2006.

853 Vaute, L., Drogue, C., Garrelly, L. and Ghelfenstein, M.: Relations between the structure of
854 storage and the transport of chemical compounds in karstic aquifers, *J. Hydrol.*, 199, 221–
855 238, 1997.

856 Vita, P. De, Allocca, V., Manna, F. and Fabbrocino, S.: Coupled decadal variability of the
857 North Atlantic Oscillation , regional rainfall and karst spring discharges in the Campania
858 region (southern Italy), , 1389–1399, doi:10.5194/hess-16-1389-2012, 2012.

859 Viviroli, D., Dürr, H. H., Messerli, B., Meybeck, M. and Weingartner, R.: Mountains of the
860 world, water towers for humanity: Typology, mapping, and global significance, *Water*
861 *Resour. Res.*, 43(7), W07447, doi:10.1029/2006WR005653, 2007.

862 De Vries, J. J. and Simmers, I.: Groundwater recharge: an overview of processes and
863 challenges, *Hydrogeol. J.*, 10(1), 5–17, doi:10.1007/s10040-001-0171-7, 2002.

864 Wada, Y., van Beek, L. P. H., van Kempen, C. M., Reckman, J. W. T. M., Vasak, S. and
865 Bierkens, M. F. P.: Global depletion of groundwater resources, *Geophys. Res. Lett.*, 37(20),
866 L20402, doi:10.1029/2010gl044571, 2010.

867 Wada, Y., Wisser, D. and Bierkens, M. F. P.: Global modeling of withdrawal, allocation and
868 consumptive use of surface water and groundwater resources, *Earth Syst. Dyn.*, 5(1), 15–40,
869 doi:10.5194/esd-5-15-2014, 2014.

870 Wagener, T., Sivapalan, M., Troch, P. A., McGlynn, B. L., Harman, C. J., Gupta, H. V.,
871 Kumar, P., Rao, P. S. C., Basu, N. B. and Wilson, J. S.: The future of hydrology: An evolving
872 science for a changing world, *Water Resour. Res.*, 46(5), W05301,
873 doi:10.1029/2009wr008906, 2010.

874 Wellings, S. R.: Recharge of the Upper Chalk aquifer at a site in Hampshire, England, *J.*
875 *Hydrol.*, 69, 275–285, doi:10.1016/0022-1694(84)90167-7, 1984.

876 Wigington, P. J., Leibowitz, S. G., Comeleo, R. L. and Ebersole, J. L.: OREGON
877 HYDROLOGIC LANDSCAPES : A CLASSIFICATION FRAMEWORK 1, *J. Am. Water*
878 *Resour. Assoc.*, 49(1), 163–182, doi:10.1111/jawr.12009, 2013.

879 Williams, P. W.: The role of the Subcutaneous zone in karst hydrology, *J. Hydrol.*, 61, 45–67,
880 1983.

881 Williams, P. W. and Ford, D. C.: Global distribution of carbonate rocks, *Zeitschrift für*
882 *Geomorphol.*, Suppl. 147, 1–2, 2006.

883 Winter, T. C.: The Concept of Hydrologic Landscapes, *JAWRA J. Am. Water Resour.*
884 *Assoc.*, 37(2), 335–349, doi:10.1111/j.1752-1688.2001.tb00973.x, 2001.

885 Wood, E. F., Roundy, J. K., Troy, T. J., van Beek, L. P. H., Bierkens, M. F. P., Blyth, E., de
886 Roo, A., Döll, P., Ek, M., Famiglietti, J., Gochis, D., van de Giesen, N., Houser, P., Jaffé, P.

887 R., Kollet, S., Lehner, B., Lettenmaier, D. P., Peters-Lidard, C., Sivapalan, M., Sheffield, J.,
888 Wade, A. and Whitehead, P.: Hyperresolution global land surface modeling: Meeting a grand
889 challenge for monitoring Earth's terrestrial water, *Water Resour. Res.*, 47(5), W05301,
890 doi:10.1029/2010WR010090, 2011.

891 Zagana, E., Tserolas, P., Floros, G., Katsanou, K. and Andreo, B.: First outcomes from
892 groundwater recharge estimation in evaporate aquifer in Greece with the use of APLIS
893 method, in *Advances in the Research of Aquatic Environment*, edited by N. Lambrakis, G.
894 Stournaras, and K. Katsanou, pp. 89–96, Springer Berlin Heidelberg., 2011.

895

896

Tables

Table 1: Data availability, data properties and sources

Variable	Spatial resolution	Time period	Frequency	Source	Reference
Precipitation	0.25°	2002-2012	daily	GLDAS-2	(Rodell et al., 2004; Rui and Beaudoin, 2013)
Temperature	0.25°	2002-2012	daily	GLDAS-2	
Net radiation	0.25°	2002-2012	daily	GLDAS-2	
Snow water equivalent	0.25°	2002-2012	daily	NOAHv3.3 /GLDAS-2	(Ek, 2003; Rodell et al., 2004)
Carbonate rock areas	vector data	-	-		(Williams and Ford, 2006)
Elevation	3''	-	-	SRMT V2.1	(USGS, 2006)
Rock permeability	vector data	-	-		(Gleeson et al., 2014a)
Actual evaporation	individual locations	individual periods	daily	FLUXNET	(Baldocchi et al., 2001)
Soil moisture	Individual locations	individual periods	daily	ISMN	(Dorigo et al., 2011)

Table 2: ~~Parameter~~Parameter description and ~~Initial parameter~~ ranges for Monte Carlo sampling based on previous field studies and large-scale model applications

Parameter	Unit	Description	Lower Limit*	Upper limit*	References
α	[-]	<u>Variability constant</u>	0	6	(Hartmann et al., 2013b, 2014c, 2015)
V_{soil}	[mm]	<u>Mean soil storage capacity</u>	0	1250	(Miralles et al., 2011; FAO/IIASA/ISRIC/ISSCAS/JRCv, 2012; Ek, 2003)
V_{epi}	[mm]	<u>Mean epikarst storage capacity</u>	200	700	(Perrin et al., 2003; Williams, 2008)
K_{epi}	[d]	<u>Mean epikarst storage coefficient</u>	0	50	(Gleeson et al., 2014b; Hartmann et al., 2013b)

Table 3: Independent observations of mean annual recharge from field and modelling studies over Europe and the Mediterranean

<u>Location</u>	<u>Latitude</u>	<u>Longitude</u>	<u>Mean annual recharge</u>	<u>Method</u>	<u>Author</u>
<u>(country, province)</u>	<u>[dec. degr.]</u>	<u>[dec. degr.]</u>	<u>[mm]</u>		
<u>Austria (Siebenquellen spring, Schneeaple)</u>	<u>47.69</u>	<u>15.6</u>	<u>694</u>	<u>observed water balance</u>	<u>(Maloszewski et al., 2002)</u>
<u>Croatia (Jadro spring, Dugopolje)</u>	<u>43.58</u>	<u>16.6</u>	<u>795</u>	<u>simulated water balance</u>	<u>(Jukic and Denic-Jukic, 2008)</u>
<u>Croatia (St. Ivan, Mirna)</u>	<u>45.22</u>	<u>13.6</u>	<u>386</u>	<u>observed water balance</u>	<u>(Bonacci, 2001)</u>
<u>France (Bonnieure, La Rouchefoucauld-Touvre)</u>	<u>45.8</u>	<u>0.44</u>	<u>250</u>	<u>simulated water balance</u>	<u>(Le Moine et al., 2007)</u>
<u>France (Durzon spring, La Cavalerie)</u>	<u>44.01</u>	<u>3.16</u>	<u>378</u>	<u>observed water balance</u>	<u>(Tritz et al., 2011)</u>
<u>France (Fontaine de Vaucluse)</u>	<u>43.92</u>	<u>5.13</u>	<u>568</u>	<u>observed water balance</u>	<u>(Fleury et al., 2007)</u>
<u>France (St Hippolyte-du-Fort, Vidourle)</u>	<u>43.93</u>	<u>3.85</u>	<u>287</u>	<u>observed water balance</u>	<u>(Vaute et al., 1997)</u>
<u>Germany (Bohming spring, Rieshofen)</u>	<u>48.93</u>	<u>11.3</u>	<u>130</u>	<u>observed water balance</u>	<u>(Einsiedl, 2005)</u>
<u>Germany (Gallusquelle spring, Swabian Albs)</u>	<u>48.21</u>	<u>9.15</u>	<u>351</u>	<u>observed water balance</u>	<u>(Doummar et al., 2012)</u>
<u>Germany (Hohenfells)</u>	<u>49.2</u>	<u>11.8</u>	<u>200</u>	<u>observed water balance</u>	<u>(Quinn et al., 2006)</u>
<u>Greece (Arvi, Crete)*</u>	<u>35.13</u>	<u>24.55</u>	<u>241</u>	<u>observed water balance</u>	<u>(Koutroulis et al., 2013)</u>
<u>Greece (Aitolokarnania)</u>	<u>38.60</u>	<u>21.15</u>	<u>484</u>	<u>empiric estimation method</u>	<u>(Zagana et al., 2011)</u>
<u>Italy (Cerella spring, Latina)</u>	<u>41.88</u>	<u>12.9</u>	<u>416</u>	<u>empiric estimation method</u>	<u>(Allocca et al., 2014)</u>
<u>Italy (Forcella spring, Sapri)</u>	<u>41.05</u>	<u>14.55</u>	<u>559</u>	<u>empiric estimation method</u>	<u>(Allocca et al., 2014)</u>
<u>Italy (Gran Sasso, Teramo)</u>	<u>42.27</u>	<u>13.34</u>	<u>700</u>	<u>observed water balance</u>	<u>(Barbieri et al., 2005)</u>
<u>Italy (Sanità)</u>	<u>40.78</u>	<u>15.13</u>	<u>974</u>	<u>observed water balance</u>	<u>(Vita et al., 2012)</u>
<u>Italy (Taburno spring)</u>	<u>39.9</u>	<u>15.81</u>	<u>693</u>	<u>empiric estimation method</u>	<u>(Allocca et al., 2014)</u>
<u>Lebanon (Anjar-Chamsine)</u>	<u>33.73</u>	<u>35.93</u>	<u>278</u>	<u>observed water balance</u>	<u>(Bakalowicz et al., 2008)</u>
<u>Lebanon (Zarka)</u>	<u>34.08</u>	<u>36.30</u>	<u>205</u>	<u>observed water balance</u>	<u>(Bakalowicz et al., 2008)</u>
<u>Lebanon (Afka)</u>	<u>34.05</u>	<u>35.95</u>	<u>842</u>	<u>observed water balance</u>	<u>(Bakalowicz et al., 2008)</u>
<u>Palestine (Mountain Aquifer)</u>	<u>~32.00</u>	<u>~35.30</u>	<u>144</u>	<u>simulated water balance</u>	<u>(Hughes et al., 2008)</u>
<u>Portugal (Algarve, minimum value)</u>	<u>~37.10</u>	<u>~-7.90</u>	<u>130</u>	<u>not mentioned</u>	<u>(de Vries and Simmers, 2002)</u>
<u>Portugal (Algarve, maximum value)</u>	<u>~37.10</u>	<u>~-7.90</u>	<u>300</u>	<u>not mentioned</u>	<u>(de Vries and Simmers, 2002)</u>
<u>Saudi Arabia (Eastern Arabian peninsula)</u>	<u>~26.50</u>	<u>~46.50</u>	<u>44</u>	<u>natural tracers</u>	<u>(Hoetzel, 1995)</u>
<u>Spain (Cazorla, Sierra de Cazorla)</u>	<u>37.9</u>	<u>-3.03</u>	<u>244</u>	<u>empiric estimation method</u>	<u>(Andreo et al., 2008)</u>
<u>Spain (La Villa spring, El Torcel)</u>	<u>36.93</u>	<u>-4.52</u>	<u>463</u>	<u>observed water balance</u>	<u>(Padilla et al., 1994)</u>
<u>Spain (Sierra de las Cabras, Arcos de la frontera)</u>	<u>36.65</u>	<u>-5.72</u>	<u>318</u>	<u>empiric estimation method</u>	<u>(Andreo et al., 2008)</u>
<u>Switzerland (Rappenfluh Spring)</u>	<u>47.87</u>	<u>7.67</u>	<u>650</u>	<u>simulated water balance</u>	<u>(Butscher and Huggenberger, 2008)</u>
<u>Turkey (Aydincik, Mersin)</u>	<u>36.97</u>	<u>33.22</u>	<u>552</u>	<u>observed water balance</u>	<u>(Hatipoglu-Bagci and Sazan, 2014)</u>
<u>Turkey (Harmankoy, Beyyayla)</u>	<u>40.15</u>	<u>30.65</u>	<u>32</u>	<u>observed water balance</u>	<u>(Aydin et al., 2013)</u>
<u>UK (Marlborough and Berkshire Downs and South-West Chilterns,</u>	<u>51.53</u>	<u>-1.15</u>	<u>146</u>	<u>simulated water balance</u>	<u>(Jackson et al., 2010)</u>

<u>minimum value)</u>					
<u>UK (Marlborough and Berkshire Downs and South-West Chilterns, maximum value)</u>	<u>51.53</u>	<u>-1.15</u>	<u>365</u>	<u>simulated water balance</u>	<u>(Jackson et al., 2010)</u>
<u>UK (Dorset)</u>	<u>50.75</u>	<u>-2.45</u>	<u>700</u>	<u>observed water balance</u>	<u>(Foster, 1998)</u>
<u>UK (Norfolk)</u>	<u>52.60</u>	<u>0.88</u>	<u>260</u>	<u>observed water balance</u>	<u>(Foster, 1998)</u>
<u>UK (Greta spring, Durham)</u>	<u>54.52</u>	<u>-1.87</u>	<u>690</u>	<u>observed water balance</u>	<u>(Arnell, 2003)</u>
<u>UK(R. Teme, Tenbury wells)</u>	<u>52.3</u>	<u>-2.58</u>	<u>355</u>	<u>observed water balance</u>	<u>(Arnell, 2003)</u>
<u>UK(Lambourn)</u>	<u>51.5</u>	<u>-1.53</u>	<u>234</u>	<u>observed water balance</u>	<u>(Arnell, 2003)</u>
<u>UK (Hampshire)</u>	<u>51.1</u>	<u>-1.26</u>	<u>348</u>	<u>observed water balance</u>	<u>(Wellings, 1984)</u>

Table 4: Cluster means of the 4 identified karst landscapes (AI: aridity index, DS mean annual number of days with snow cover, RA: range of altitudes)

descriptor	unit	number of cluster/karst landscape			
		1.HUM	2.MTN	3.MED	4.DES
AI	[-]	0.80	0.98	3.18	20.00
DS	[a-1]	85	76	16	1
RA	[m]	228	1785	691	232

912
913

914
915
916
917

918
919
920

Table 5: Minima and maxima of the confined parameter samples for each of the identified landscapes

Parameter	Unit	HUM		MTN		MED		DES	
		min	max	min	max	min	max	min	max
a	[-]	1.1	3.3	0.3	2.9	0.8	6.0	0.1	6.0
V_{soil}^*	[mm]	900.1 (900)	1248.9 (1250)	500.4 (500)	899.9 (900)	51.7 (50)	498.4 (500)	0.2 (0)	49.1 (500)
V_{epi}	[mm]	204.3	694.8	201.6	699.4	200.1	696.7	202.3	695.7
K_{epi}	[d]	0.0	35.8	7.3	49.9	0.0	48.4	10.4	49.9

* in brackets: *a priori* information used for step 3 of the parameter confinement strategy

Table 6: Mean deviations of the VarKarst-R, the PCR-GLOBWB model and the WaterGAP model from all observations and the individual regions

region	mean deviation [mm/a]		
	VarKarst-R	PCR-GLOBWB	WaterGAP
all	-58.3	-230.4	-264.2
HUM	65.5	-90.2	-151.6
MTN	-202.8	-427.5	-446.4
MED	-4.3	-217.3	-211.4

Figures

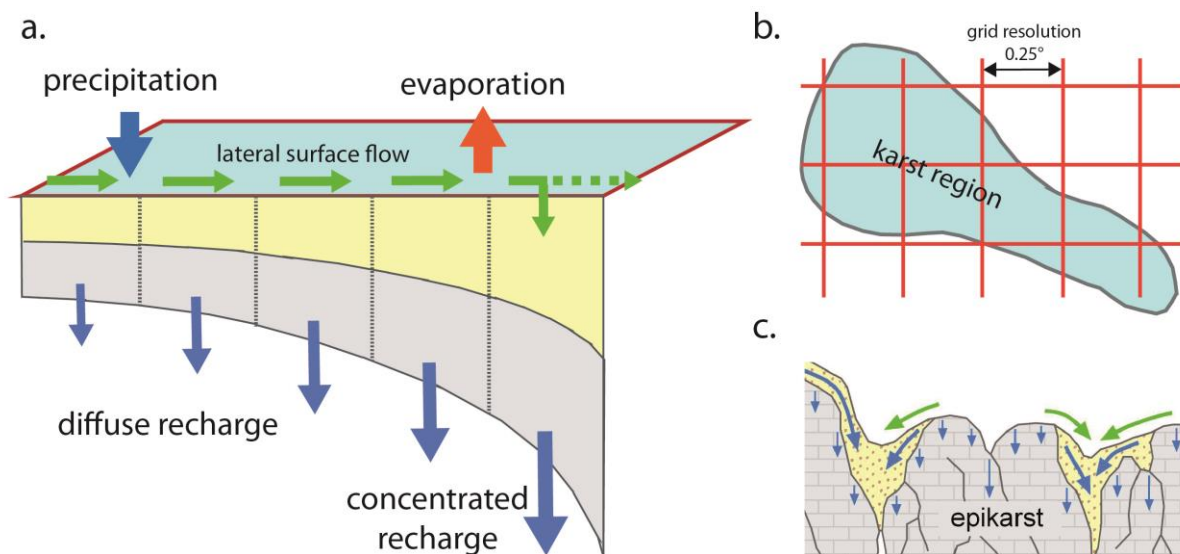


Figure 1: (a) schematic description of the model for one grid cell including the soil (yellow) and epikarst storages (grey) and the simulated fluxes, (b) its gridded discretisation over karst regions and (c) the subsurface heterogeneity that its structure represents for each grid cell.

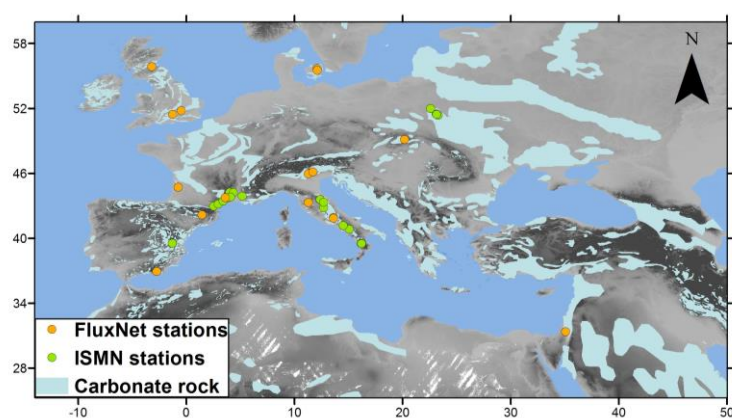


Figure 2: Carbonate rock areas over Europe and the Mediterranean, and location of the selected FLUXNET and ISMN stations

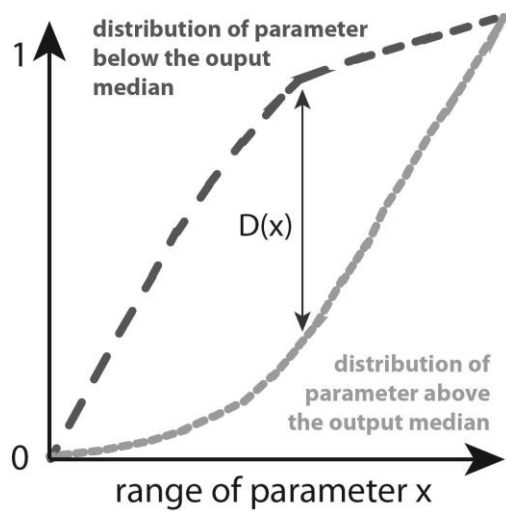


Figure 3: Schematic elaboration of the regional sensitivity analysis procedure

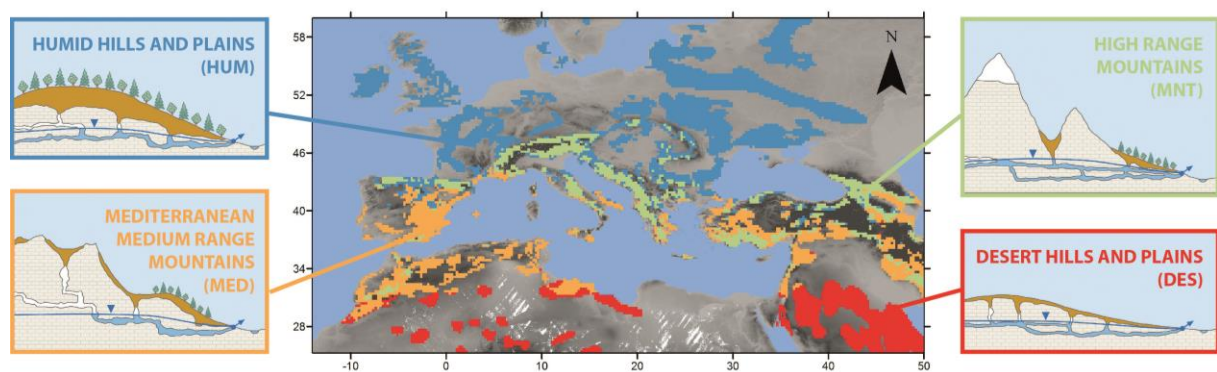


Figure 4: Map with clusters over Europe and typical karst landscapes that were attributed to them

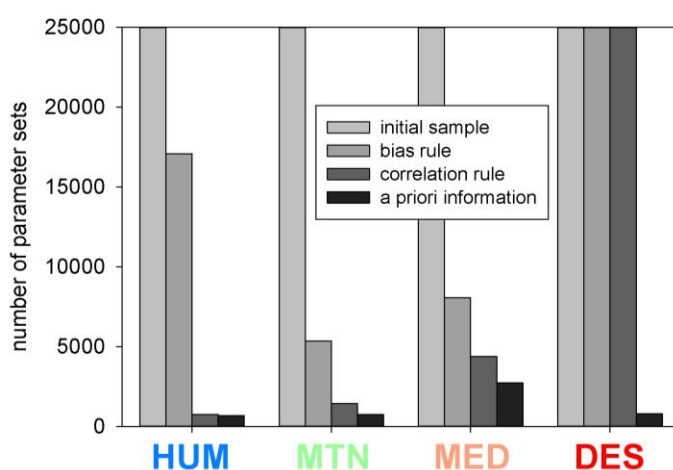


Figure 5: Evolution of the initial sample of 25,000 parameter sets (each including the 4 model parameters sampled from within their initial ranges) along the different confinement steps for the 4 karst landscapes

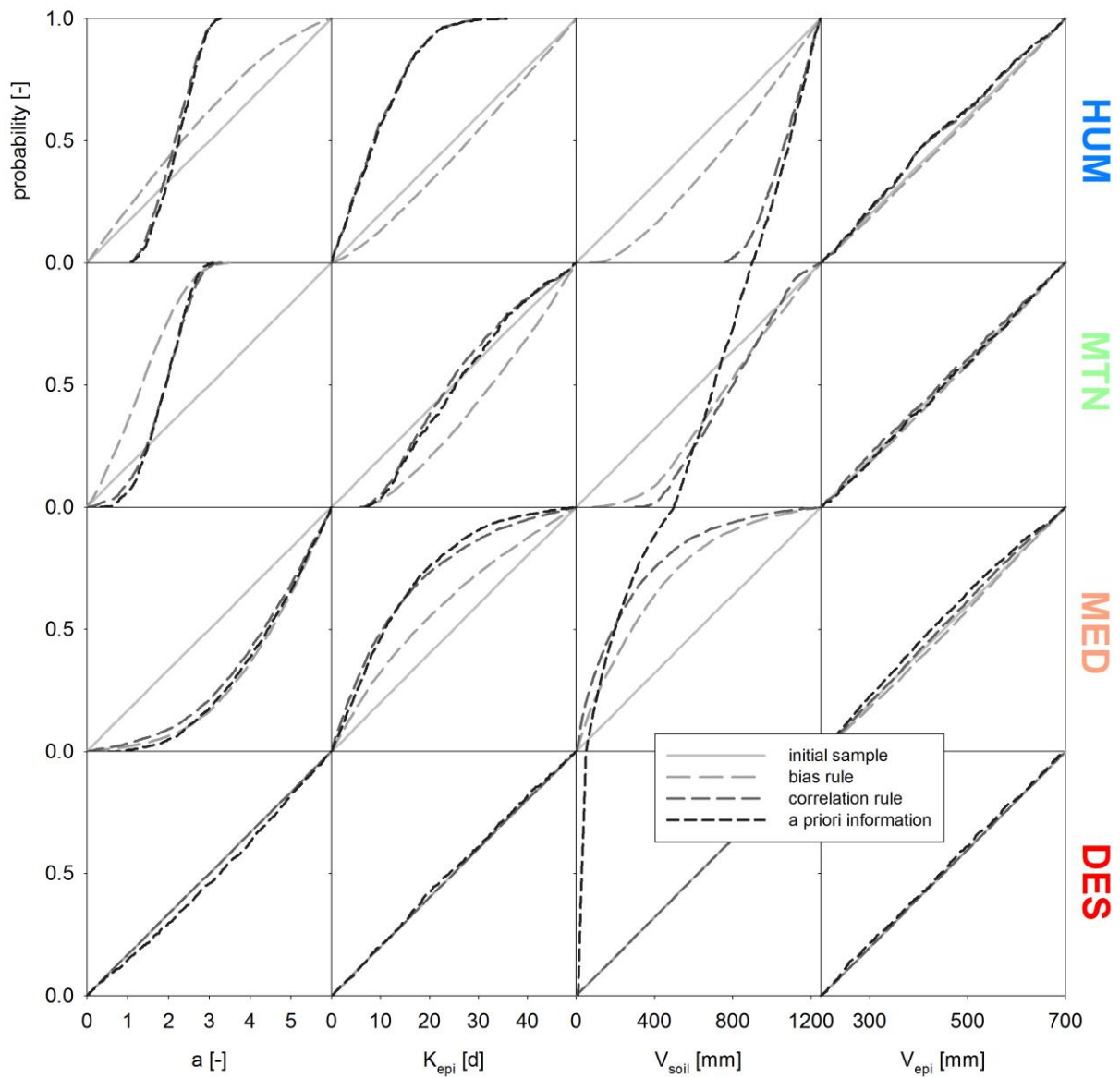


Figure 6: Evolution of *posterior* probabilities of the 4 model parameters for the 4 karst landscapes along the steps of the parameter confinement strategy.

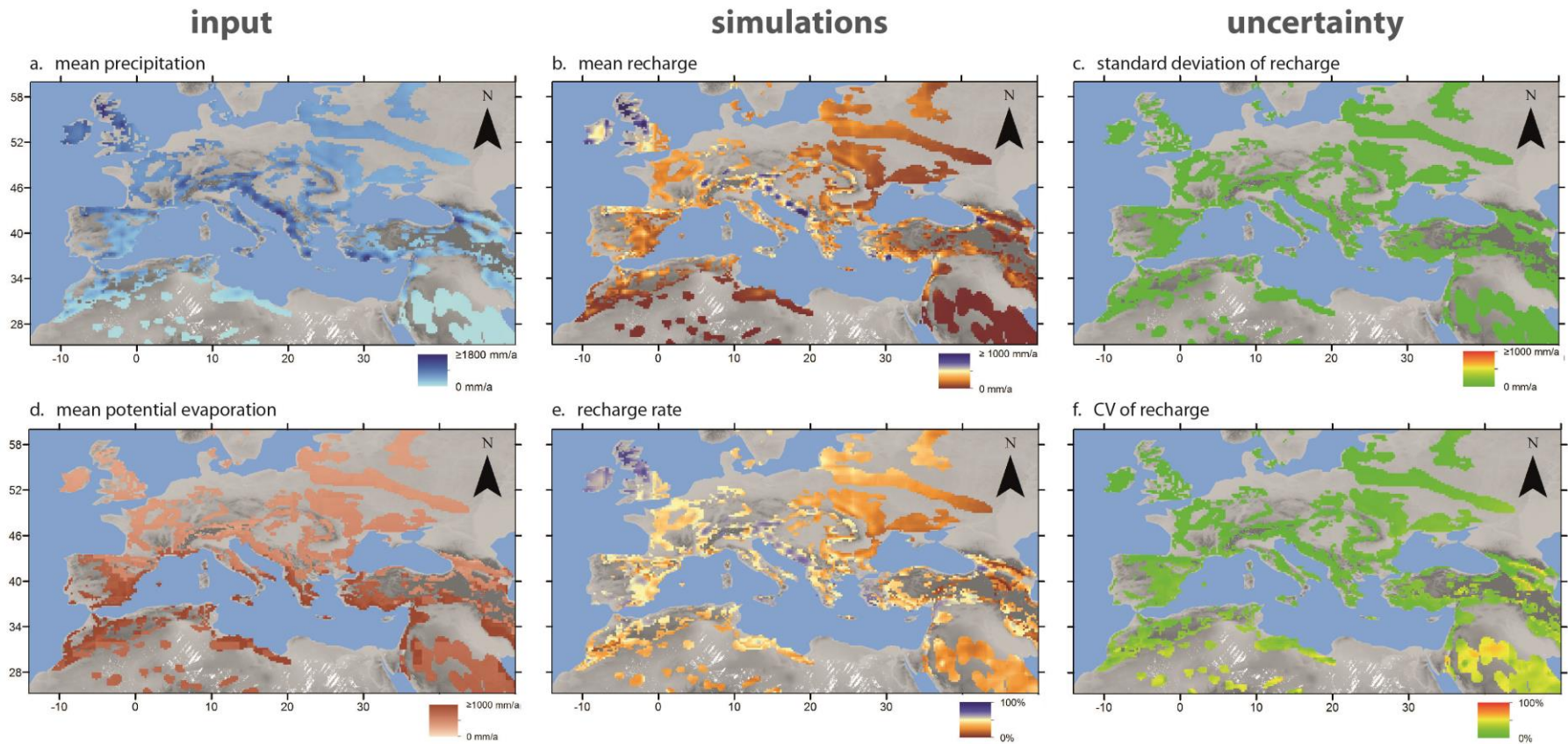


Figure 7: (a) Observed precipitation and (d) potential evaporation versus the simulated (b) mean annual recharge and (e) mean annual recharge rates derived from the mean of all 250 parameter sets, and (c) the standard deviation and (f) coefficients of variation of the simulations due to the variability among the 250 parameter sets.

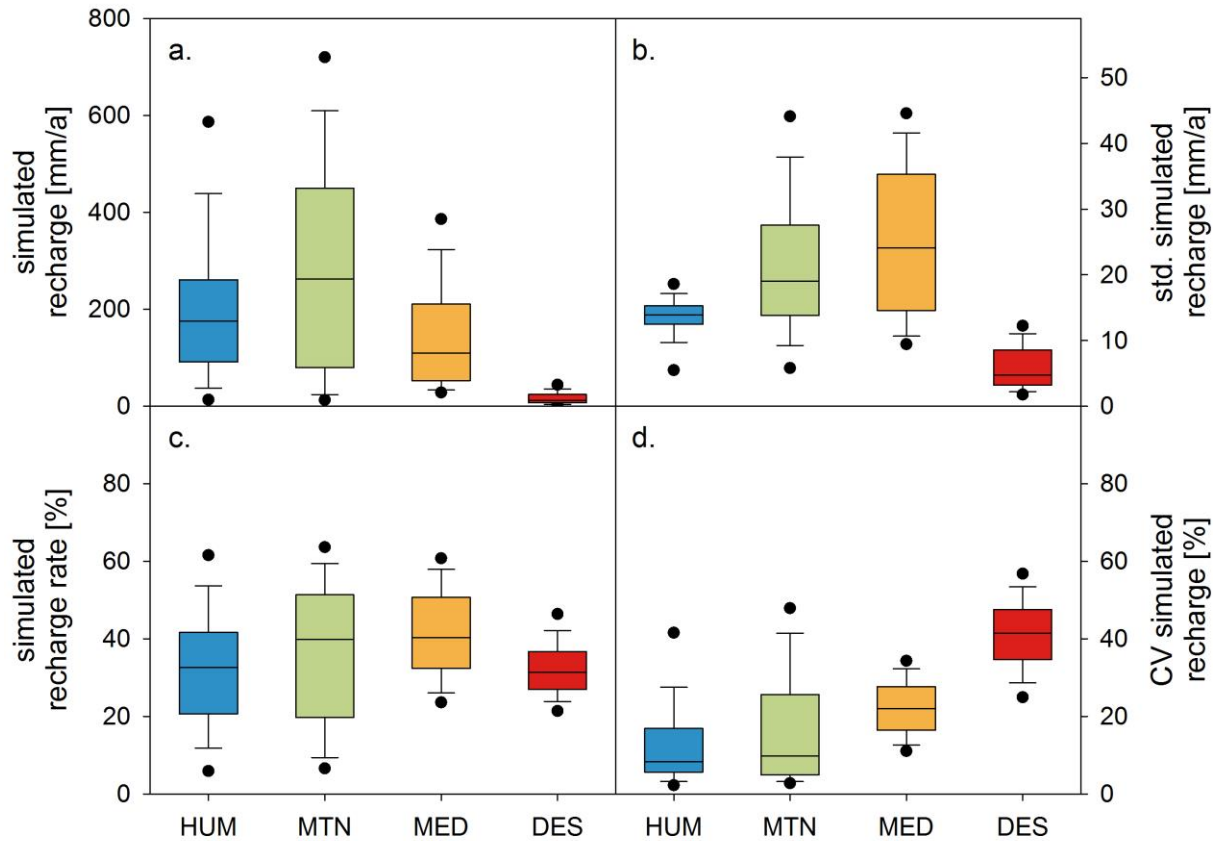


Figure 8: (a) Simulated mean annual recharge, among the 4 karst landscapes, (b) their standard deviations, (c) recharge rates, and (d) coefficients of variation obtained by the final sample of parameters.

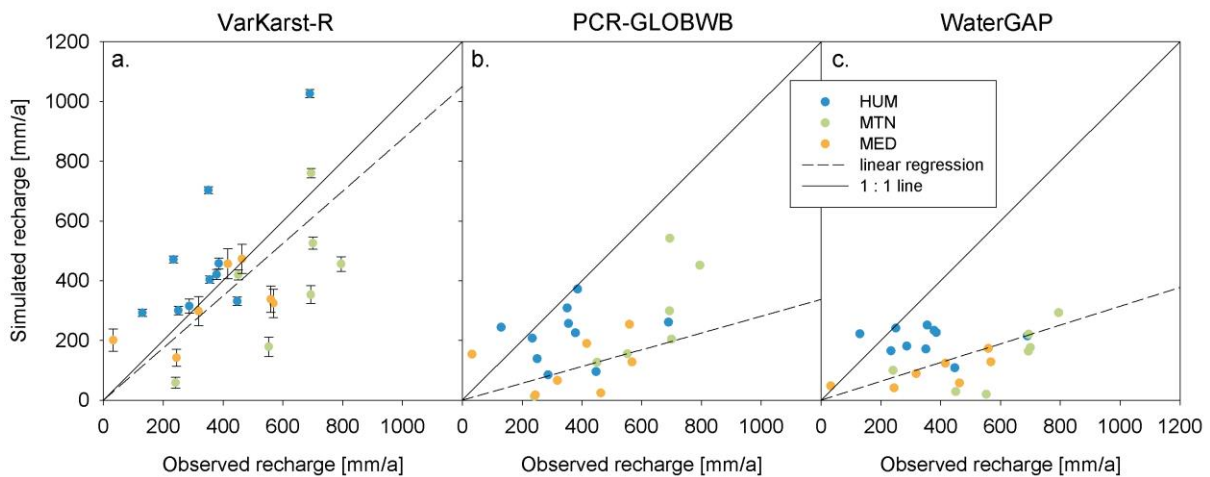


Figure 9: Observations of mean annual recharge from independent studies (Table 3) versus the simulated mean annual recharge by the VarKarst-R and the PCR-GLOBWB model (no data for the DES region available)

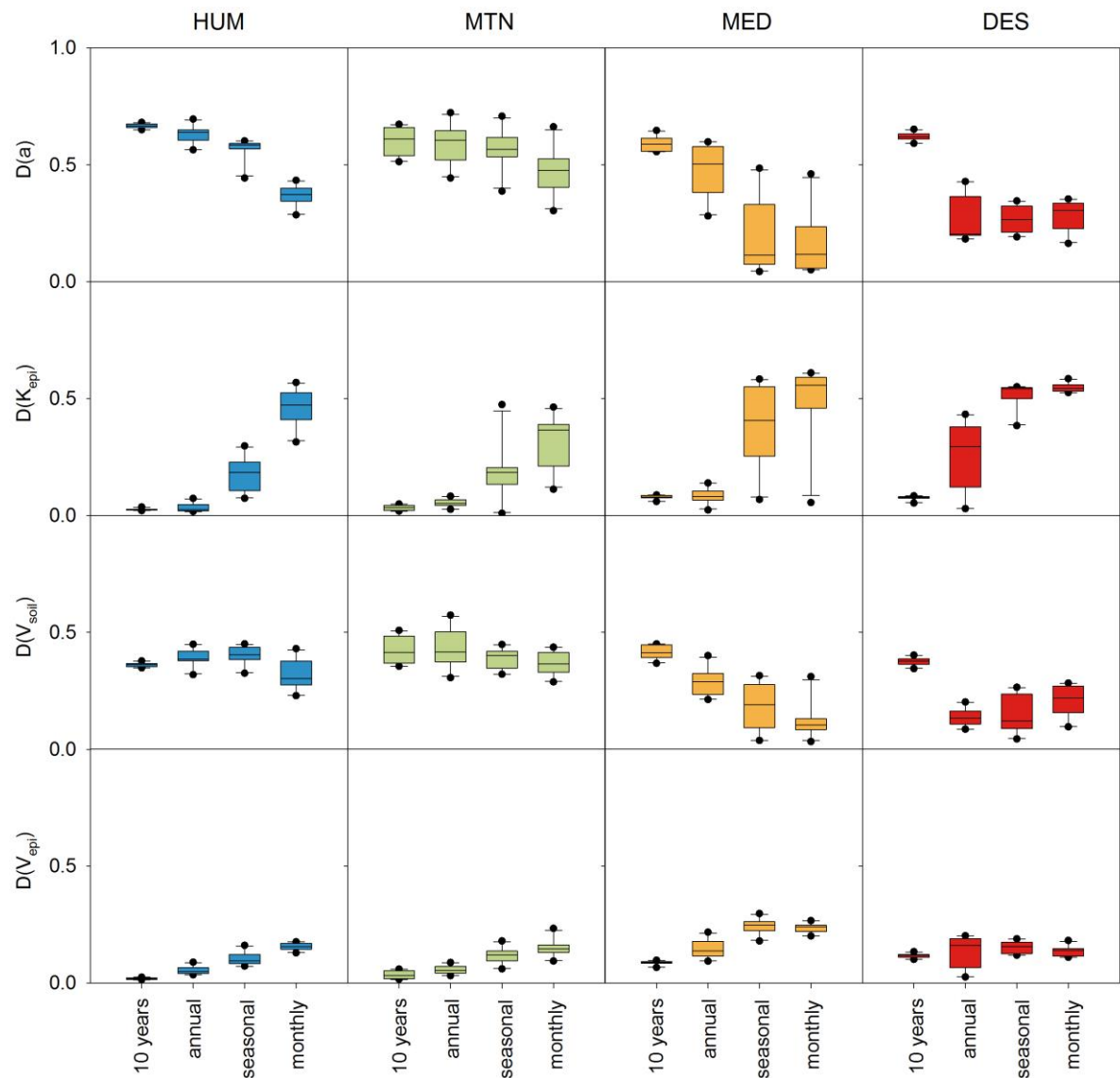
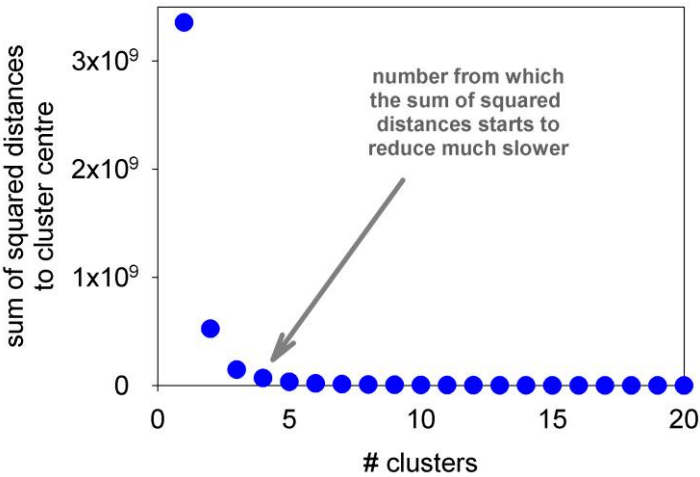


Figure 10: Sensitivity of simulated recharge to the model parameters at different time scales and in the different karst landscapes. Sensitivity is measured by the maximum distance (D) between the distribution of parameter sets that produce ‘low’ recharge (i.e. below the median) and the distribution producing ‘high’ recharge (above the median). Parameter sets are initially sampled from the ranges in Table 2.

963 **6 Appendix**

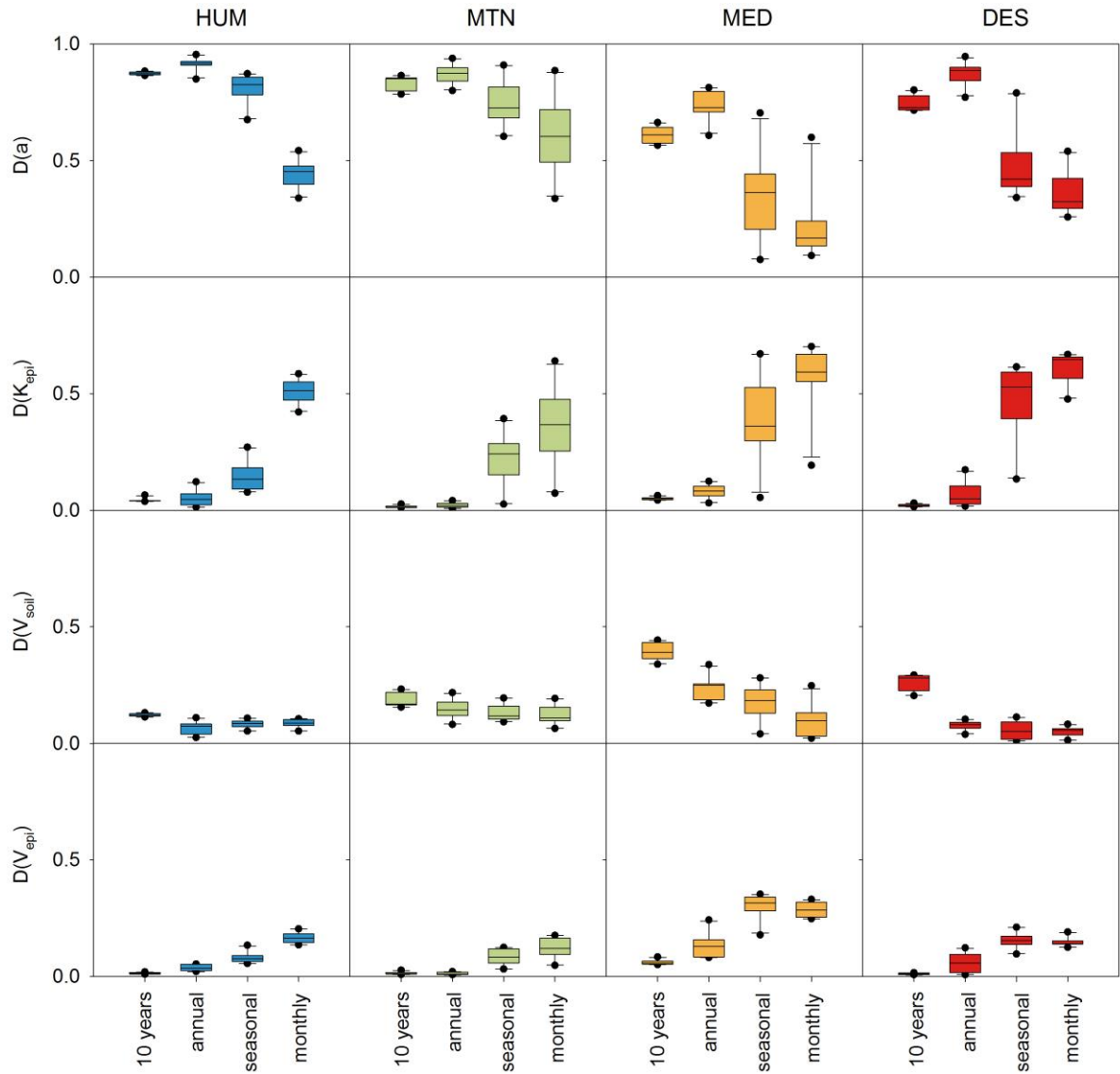
964 **6.1 Results of the cluster analysis**



965

966 **Figure A 1: Elbow plot of sum of squared distances to cluster centres for k-means method**

967 **6.2 Results of the regional sensitivity using initial ranges**



968
969 Figure A 2: Sensitivity of simulated recharge to the model parameters at different time scales
970 and in the different karst landscapes, as in Figure 10 but sampling parameters from the
971 confined parameter ranges of [Table 5Table 5](#)